EBioMedicine 73 (2021) 103641

Contents lists available at ScienceDirect

EBioMedicine

journal homepage: www.elsevier.com/locate/ebiom

# Metallothionein 2 activation by pravastatin reinforces epithelial integrity and ameliorates radiation-induced enteropathy

Seo Young Kwak[a], Won Il Jang[a], Seungwoo Park[b], Sang Sik Cho[a,c], Seung Bum Lee[a], Min-Jung Kim[a], Sunhoo Park[a], Sehwan Shim[a,*,**,1], Hyosun Jang[a,*,**,1]

[a] Laboratory of Radiation Exposure & Therapeutics, National Radiation Emergency Medical Center, Korea Institute of Radiological and Medical Sciences, Seoul 01812, Republic of Korea
[b] Comprehensive Radiation Irradiation Center, Korea Institute of Radiological and Medical Sciences, Seoul 01812, Republic of Korea
[c] Department of Surgery, Korea Institute of Radiological and Medical Sciences, Seoul 01812, Republic of Korea

ARTICLE INFO

*Article History:*
Received 29 June 2021
Revised 5 October 2021
Accepted 7 October 2021
Available online xxx

*Key words:*
Radiation-induced enteropathy
Epithelial integrity
Pravastatin
Minipigs
Metallothionein 2

ABSTRACT

*Background:* Radiotherapy or accidental exposure to ionizing radiation causes severe damage of healthy intestinal tissues. Intestinal barrier function is highly sensitive to ionizing radiation, and loss of epithelial integrity results in mucosal inflammation, bacterial translocation, and endotoxemia. Few studies have of epithelial integrity as a therapeutic target to treat radiation toxicity. Here, we examined the effects of pravastatin (PS) and the molecular mechanisms underlying epithelial integrity on radiation-induced enteropathy.
*Methods:* The radio-mitigative effects of PS were evaluated in a minipig model by quantifying clinical symptoms, and performing histological and serological analyses and mRNA sequencing in intestinal tissues. To evaluate the role of intercellular junctions on radiation damage, we used tight junction regulator and metallothionein 2 (MT2) as treatments in a mouse model of radiation-induced enteropathy. Caco-2 monolayers were used to examine functional epithelial integrityand intercellular junction expression.
*Finding:* Using a minipig model of pharmaceutical oral bioavailability, we found that PS mitigated acute radiation-induced enteropathy. PS-treated irradiated minipigs had mild clinical symptoms, lower intestinal inflammation and endotoxin levels, and improved gastrointestinal integrity, compared with control group animals. The results of mRNA sequencing analysis indicated that PS treatment markedly influenced intercellular junctions by inhibiting p38 MAPK signaling in the irradiated intestinal epithelium. The PS-regulated gene MT2 improved the epithelial barrier via enhancement of intercellular junctions in radiation-induced enteropathy.
*Interpretation:* PS regulated epithelial integrity by modulating MT2 in radiation-damaged epithelial cells. These findings suggested that maintenance of epithelial integrity is a novel therapeutic target for treatment of radiation-induced gastrointestinal damage.
*Funding:* As stated in the Acknowledgments



## 1. Introduction

The epithelial barrier is the first line of defense in the gastrointestinal (GI) tract to prevent excessive exposure of mucosal tissue to microbial antigens and external pathogens. Epithelial barrier dysfunction leads to mucosal inflammation with inflammatory cell recruitment, bacterial translocation, and endotoxemia [1]. Intercellular junctions of epithelial cells include adherens junctions (AJs), tight junctions (TJs), and desmosomes. These critical components of the epithelial barrier maintain intestinal homeostasis by regulating paracellular permeability and epithelial integrity [2]. Uncontrolled intestinal permeability can increase susceptibility to develop external stimuli-associated intestinal inflammation [3]. Clinical evidence also suggests that increased intestinal barrier dysfunction is a risk factor for GI disease because disturbance of epithelial integrity is typically present before inflammatory bowel disease (IBD) onset in human subjects [4]. Damaged mucosa from IBD patients has characteristics of altered intercellular junction structure and epithelial permeability [5].

* **Corresponding authors**: Hyosun Jang, PhD, DVM, Laboratory of Radiation Exposure & Therapeutics, National Radiation Emergency Medical Center, Korea Institute of Radiological and Medical Sciences (KIRAMS), 75 Nowon-ro, Nowon-gu, Seoul 01812, Republic of Korea
** Sehwan Shim, PhD, DVM, Laboratory of Radiation Exposure & Therapeutics, National Radiation Emergency Medical Center, Korea Institute of Radiological and Medical Sciences (KIRAMS), 75 Nowon-ro, Nowon-gu, Seoul 01812, Republic of Korea
*E-mail addresses:* ssh3002@kirams.re.kr (S. Shim), hsjang@kirams.re.kr (H. Jang).
[1] Corresponding authors contributed equally to this work.

https://doi.org/10.1016/j.ebiom.2021.103641

**Research in context**

*Evidence before this study*

The epithelial barrier is front line of defense in the GI tract to prevent excessive exposure of mucosal tissue to microbial antigens and external pathogens. Intercellular junctions and barrier functions of the intestinal epithelium are highly sensitive to ionizing radiation, and a disruption of junction molecules decreases the integrity of the intestinal epithelium. On the other hand, there is limited research about therapeutic targets that block the breakdown of epithelial integrity and mitigate radiation-induced enteropathy. In a previous study, we found that PS mitigated radiation-induced enteropathy and improved intestinal barrier function in a mouse model of radiation-induced enteropathy. However, the effects of PS and the molecular mechanisms underlying epithelial integrity are not fully understood.

*Added value of this study*

We demonstrated that PS mitigated radiation-induced enteropathy and improved intestinal integrity in a minipig model of pharmaceutical oral bioavailability. PS improved epithelial integrity by regulating intercellular junction molecules and inhibiting p38 MAPK after radiation-induced epithelial damage. The PS-regulated gene MT2 improved epithelial integrity and caused hyper-resistance to radiation-induced intestinal injury.

*Implications of all the available evidence*

Activation of MT2 by chemicals such as PS may have therapeutic potential for alleviating conditions in which epithelial barrier formation is compromised by irradiation. These results indicate that PS reinforces epithelial integrity by modulating MT2 after radiation-induced epithelial damage. Maintenance of epithelial integrity is a novel therapeutic target for radiation-induced GI damage.

Radiotherapy or accidental exposure to ionizing radiation causes severe damage to healthy intestinal tissues of the GI tract [6]. The GI complications of radiation exposure from dirty bombs and nuclear accidents are called GI acute radiation syndrome (GI-ARS) [7]. GI-ARS is characterized by nausea, diarrhea, endotoxemia, and bacteremia leading to septicemia [8,9]. Intestinal epithelial intercellular junctions and barrier functions are highly sensitive to ionizing radiation, and a rapid disruption of junction molecules decreases epithelial integrity in the intestine [10]. Clinical studies found that patients receiving radiotherapy have increased intestinal permeability and TJ disruption [11]. However, there is limited research about therapeutic targets to resist breakdown of epithelial integrity and mitigate radiation-induced enteropathy.

Statins inhibit 3-hydroxy-3-methylglutaryl coenzyme A reductase and are extensively used to treat hypercholesterolemia. Because the inactivation of this enzyme reduces cholesterol biosynthesis, statins reduce levels of circulating total cholesterol, low- density lipoprotein, cholesterol, and apolipoprotein B [12]. In addition to their lipid-lowering action, statins have pleiotropic effects such as anti-inflammation, anti-oxidation, and improvement of endothelial dysfunction. The statin, pravastatin (PS), has therapeutic effects on radiation-induced GI damage [13-16]. The anti-inflammatory and anti-fibrotic effects of PS use following radiation exposure have been revealed using mouse models [14-16]. One clinical study found that statin use was associated with reduced acute GI syndrome following pelvic radiotherapy [17]. Using a mouse model, we found that during GI-ARS-associated epithelial damage, PS improves epithelial barrier function in the small intestinal epithelium [13]. Administration of PS relieves dextran sodium sulfate-induced colitis by improving intestinal epithelial permeability [18]. However, the effects of PS and the molecular mechanisms underlying epithelial integrity are not fully understood.

Metallothionein (MT) is a highly conserved, low-molecular-weight, cysteine-rich protein. MT has important roles in homeostasis and detoxication of heavy metals and exhibits cytoprotection against oxidative stress-induced damage [19-21]. MT thus has protective effects against environmental stress-associated cell damage. There are four main isoforms of MT in mammals, MT1, MT2, MT3, and MT4. MT1 and MT2 are ubiquitously expressed in various tissues and are sensitive to activation by a variety of developmental and environmental signals [22,23]. MT3 and MT4 are minor isoforms with restricted expression in specialized cells and tissues, such as the brain, reproductive organs, and stratified squamous epithelium; they are constitutively expressed despite signal changes [22]. MT1- and MT2- (MT1/2-) deficient mice have sensitive responses to inflammation and external stimuli [24-26]. MT regulates pulmonary endothelial and epithelial integrity and attenuates ozone-induced lung inflammation [25]. However, there are limited reports regarding the direct role of MT in the maintenance of epithelial barrier integrity.

In this study using both minipig and mouse models, we found that PS reinforced epithelial integrity and mitigated acute radiation-induced enteropathy. PS use resulted in upregulation of intercellular junctions, and this function of PS enhanced the therapeutic effects on radiation-induced enteropathy. PS regulated MT1/2 and improved epithelial integrity via increases in numbers of intercellular junctions and inhibited p38 MAPK in irradiated Caco-2 cells. Finally, MT2 application alleviated radiation-induced intestinal injury. Taken together, these results indicated that PS reinforced epithelial integrity by modulating MT2 in radiation-damaged epithelial cells and that maintenance of epithelial integrity is a novel therapeutic target that can be used to alleviate radiation-induced GI damage.

## 2. Methods

### 2.1. Animals

#### 2.1.1. Minipigs

Six male Gottingen minipigs (PWG genetics Korea, PyungTek, Korea) weighing 20−25 kg each were used in this study. Before purchase, the minipigs were physically examined and determined to be healthy. They were housed indoors in individual cages, fed dry pig food, and provided triple-filtered water. The animals were housed under environmentally controlled conditions at 22±1°C and 50±10% relative humidity, with a 12-h light:dark cycle. All animal care was performed according to the Guide for the Care and Use of Laboratory Animals of the Institute of Laboratory Animal Resources. All animal experiments were approved by the Animal Investigation Committee of the Korea Institute of Radiological and Medical Sciences (KIRAMS, kirams 2020-0025). A total of six minipigs were used in this study. All animals analyzed were included in the results. Minipigs were randomized before starting treatment in all experiments.

#### 2.1.2. Mice

Specific pathogen-free male C57BL/6 mice (7-weeks-old) were obtained from Orient Bio (Seoul, Korea) and maintained in specific pathogen-free conditions at the KIRAMS animal facility. All mice were housed in a temperature-controlled room with a 12-h light: dark cycle. Food and water were provided ad libitum. The mice were acclimated for 1 week before commencement of the experiments and assignment to groups. All animal experiments were approved and performed in accordance with the guidelines of the Institutional Animal Care and Use Committee of the KIRAMS (kirams 2020-0069). A total of 83 mice were used in this study. All animals analyzed were

included in the results and none was excluded. Mice were randomized before starting treatment in all experiments.

### 2.2. *Irradiation and treatment* in vivo

#### 2.2.1. *Minipigs*

Minipigs were anesthetized using an intramuscular injection of 4 mg/kg Zoletil 50 (Virbac, Republic of Korea) and 2.3 mg/kg xylazine (Rompun®; Bayer Korea, Seoul, Korea). We randomly divided the minipigs into three groups. Two groups of two animals each were irradiated with 15 Gy applied to the abdomen. Two animals were used as controls. For irradiation, minipigs were irradiated bilaterally while placed in lateral recumbency. The average calculated dose rate at the center of the field was 1.6109 Gy/min. The cranial landmark was at the end of the xiphoid process. The field size was 21.6 × 21.6 cm under a $^{60}$Co gamma-ray irradiation unit (Gamma Beam 100-80, 780, Best Theratronics, Canada). The distance between the source of radiation and the abdominal skin was 80 cm. After irradiation, the minipigs were housed individually, fed dry pig food, and provided triple-filtered water. Each was treated with a twice daily oral dose of 40 mg/day pravastatin (Prastan; Yungin Pharm, Seoul, Korea) for 2 weeks. The animals were housed in environmentally controlled conditions at 22±1°C and 50±10% relative humidity, with a 12-h light:dark cycle. During the experimental period, clinical signs related to acute radiation-induced enteropathy, including diarrhea, movement, vomiting, and appetite were recorded. On days 13 and 14, the minipigs were euthanized and histological analyses were performed.

#### 2.2.2. *Mice*

Animals were anesthetized using an intraperitoneal injection of 85 mg/kg alfaxalone (Alfaxan®; Careside, Gyeonggi-do, Korea) and 10 mg/kg xylazine (Rompun®; Bayer Korea, Seoul, Korea). They were then irradiated using a single exposure of 13.5 Gy whole abdominal irradiation at a dose rate of 2 Gy/min (X-RAD 320 X-ray irradiator, Softex, Gyeonggi-do, Korea). After exposure, animals were injected with an intraperitoneal dose of 250 $\mu$g/day larazotide acetate (LA; MedchemExpress, Monmouth Junction, NJ, USA) or 10 $\mu$g/day MT2 (Enzo Life Sciences, Farmingdale, NY, USA) for 6 days. On day 6, the mice were euthanized and histological analyses wereperformed.

### 2.3. *Plasma assay*

To quantify the levels of serological c-reactive protein (CRP) (Cusabio Biotech Co., Ltd., Wuhan, China), endotoxin (Thermo Fisher Scientific, Waltham, MA, USA), and citrulline (Kamiya Biomedical Company, Seattle, WA, USA), plasma samples were analyzed using ELISA according to the manufacturer's instructions.

### 2.4. *Histological analysis of intestinal tissues*

The intestinal tissues of minipigs and mice were fixed using a 10% neutral buffered formalin solution, embedded in paraffin wax, and sectioned transversely at a thickness of 4 $\mu$m. The sections were then stained using hematoxylin and eosin. The severity of radiation-induced enteropathy was assessed based on the degree (0 = none, 1 = mild, 2 = moderate, 3 = high) of maintenance of the epithelial architecture, crypt damage, vascular enlargement, and infiltration of inflammatory cells in the lamina propria [14]. To perform immunohistochemical analyses, slides were subjected to antigen retrieval and then treated using 0.3% hydrogen peroxide in methyl alcohol for 20 min to block endogenous peroxidase activity. After three washes in PBS, the sections were blocked using 10% normal goat serum (Vector ABC Elite kit; Vector Laboratories, Burlingame, CA, USA) and incubated with anti-E-cadherin (E-Cad; Abcam, Cambridge, MA, USA, #ab15148), anti-zonula occludens-1 (ZO-1; Invitrogen, Carlsbad, CA, USA, #61-7300), anti-occludin (OCLN; Santa Cruz Biotechnology, Santa Cruz, CA, USA, #5562), anti-desmoglein 2 (DSG2; Abcam, #ab14415), anti-Ki-67 (Acris, Herford, Germany, #DRM004), and anti-villin (Abcam, #ab130751) antibodies. After three washes in PBS, the sections were incubated with a horseradish peroxidase-conjugated secondary antibody (Dako, Carpinteria, CA, USA) for 60 min. The peroxidase reaction was developed using a diaminobenzidine substrate (Dako) prepared according to the manufacturer's instructions, and the slides were counterstained with hematoxylin.

For fluorescent staining, slides were subjected to antigen retrieval and blocked using 5% goat serum containing 0.1% Triton X-100 for 30 min. The slides were incubated with specific antibodies for MT 1/2 (Invitrogen, #MAI-25479) diluted at 1:100 in PBS overnight at 4°C. After washing with PBS, slides were incubated with Alexa Fluor 488-labeled secondary antibody (Thermo Fisher Scientific) at room temperature. Finally, the samples were washed with PBS and then mounted using Vectashield HardSet mounting medium and stained with 4'6-diamidno-2-phenylindole (DAPI; 1 $\mu$g/mL, Vector Laboratories).

### 2.5. *RNA extraction, library construction, and sequencing*

RNA was extracted from ileum tissues of minipigs using the QIAzol lysis reagent (Qiagen, Hilden, Germany) and subsequently purified by column chromatography using a RNeasy mini kit (Qiagen). DNA contamination was assessed using a PicoGreen dsDNA assay kit (Thermo Fisher Scientific), and RNA quantity and quality were examined using an Agilent 2100 Bioanalyzer (Agilent Technologies, Santa Clara, CA). A cDNA library was generated using a TruSeq Stranded mRNA sample prep kit (Illumina, San Diego, CA), and transcriptome sequencing was performed using a TruSeq 3000/4000 SBS kit and HiSeq 4000 sequencer (Illumina) with 101 bp paired-end reads per sample (Macrogen, Seoul, Korea). All raw data sets were submitted to GEO (Accession number: GSE182829).

### 2.6. *Analysis of differentially expressed genes*

Sequenced cDNA fragments were mapped to the genomic DNA reference using HISAT2. StringTie was used for transcript assembly and determination of fragments per kilobase of transcript per million mapped reads (FPKM). FPKM values were used to assess the relative expression of a transcript. For the analysis of differentially expressed genes (DEGs), genes with an FPKM value of 0 in every sample were excluded, values of log2 (FPKM+1) were calculated, and quantile normalization was performed using the preprocessCore R library. Transcripts with fold-change values larger than 2, and P- values less than or equal to 0.05 were included in the analysis of DEGs. Hierarchical clustering analysis was performed using complete linkage and Euclidean distance as a measure of similarity to display DEG expression patterns. All DEG data analyses were performed using R 3.2.2 (www.r-project.org).

### 2.7. *Gene ontology and enrichment analysis*

Functional groups and pathways encompassing the DEGs were identified based on gene ontology and Kyoto Encyclopedia of Gene and Genomes (KEGG) pathway analyses using the Database for Annotation, Visualization, and Integrated Discovery.

### 2.8. *RNA extraction, reverse transcription-polymerase chain reaction (RT-PCR), and real-time RT-PCR quantification*

Harvested tissues from the small intestine were immediately snap-frozen and stored at −80°C until RNA extraction was performed. Total RNA was isolated from intestinal tissues and Caco-2 cells using the TRIzol reagent (Invitrogen). cDNA was synthesized

using the AccuPower RT premix (Bioneer, Daejeon, Korea) according to the manufacturer's protocol. Real-time RT-PCR was performed using a LightCycler 480 system (Roche, Basel, Switzerland). The primer sequences are provided in Supplementary Table 1. The expression levels of each target gene, determined using LightCycler 480 system software (Roche), were normalized to those of glyceraldehyde 3-phosphate dehydrogenase. Cycle threshold values were used to calculate relative mRNA expression using the $2^{-\Delta\Delta Ct}$ method.

### 2.9. Bacterial translocation assay

To evaluate bacterial translocation from the intestinal lumen to the lymph nodes, mesenteric lymph nodes were harvested from mice under sterile conditions on day 6 following irradiation. The supernatant of the lymph node homogenate was spread onto MacConkey agar (BD Biosciences, Palo Alto, CA, USA) and incubated at 37°C overnight. Colony-positive plates were then counted.

### 2.10. Cell culture

Caco-2 cells were used as an in vitro model of the intestinal epithelium, as previously described (Schlegel et al., 2010). Mycoplasma testing was performed to confirm the lack of contamination. Cells were maintained in Dulbecco's Modified Eagle Medium (Gibco, Grand Island, NY, USA) supplemented with 1% penicillin/streptomycin, and 10% fetal bovine serum (Gibco) in a humidified atmosphere at 37°C with 5% $CO_2$. Confluent cell monolayers were used for the in vitro experiments [27,28].

### 2.11. Irradiation and treatment in vitro

Seeded cells were grown for 5 days to allow for expression of differentiation traits. They were then exposed to a single 15 Gy dose using a $^{137}$Cs gamma-ray source (Atomic Energy of Canada, Ltd, Canada) and a dose rate of 3.81 Gy/min (Gammacell 3000 Elan, MDS Nordion, Ottawa, Canada). The cells were then immediately treated using PS (Sigma-Aldrich, St. Louis, MO, USA), MT1 (Enzo Life Sciences, Farmingdale, NY, USA), or MT2 (Enzo Life Sciences) for 48 h. Gene silencing was performed using either si-MT2 (Santa Cruz Biotechnology) or si-control. The si-MT2 and si-control-treated cells (final RNA concentration 100 nM) were reverse-transfected using Lipofectamine 2000 according to the manufacturer's instructions.

### 2.12. Transepithelial electrical resistance (TEER) measurement

The EVOM system (WPI, Sarasota, FL, USA) was used to measure the TEER values of epithelial monolayers. Briefly, Caco-2 cells ($1 \times 10^6$) were seeded onto 12-mm Costar Transwell filters (0.4-$\mu$m pore size, Corning, Corning, NY, USA) to form confluent epithelial monolayers. After 21 days, the cells were exposed to radiation and then treated with PS, MT1, or MT2.

### 2.13. FITC-dextran assay

Caco-2 cells were seeded onto 12-mm Costar Transwell filters (0.4-$\mu$m pore size, Corning) and grown for 21 days. After exposure to radiation, the apical sides of the monolayers that had been treated with PS, MT1, or MT2 were examined using 500 $\mu$g/mL FITC-dextran (4 kDa, Sigma-Aldrich). Fluorescent intensities of the lower chambers were measured using a fluorescence microplate reader. The excitation and emission wavelengths used were 450 and 520 nm, respectively.

### 2.14. Dispase-based dissociation assay

The adhesive forces between cells were assessed using a dispase-based dissociation assay. Confluent Caco-2 cells were exposed to radiation, and immediately treated with PS or MT2 for 48 h. The cells were washed twice with PBS and incubated in dispase II (2.4 units/mL, Roche) and collagenase type I (Gibco) for 30 min at 37°C. The monolayers were then carefully subjected to mechanical stress using an electronic pipet, and images were obtained using a digital camera.

### 2.15. Immunofluorescence assay

Caco-2 cells were fixed in 4% paraformaldehyde were then permeabilized (0.1% triton X-100, 5% bovine serum albumin) for 1 h at room temperature. The cells were incubated (4°C) overnight with primary antibodies. After a brief washing step, the cells were incubated with Alexa Fluor 488-labeled secondary antibody (Thermo Fisher Scientific) for 1 h at room temperature. During the final step, the cells were incubated with DAPI for counterstaining and then mounted using Vectashield HardSet mounting medium (Vector Laboratories). Fluorescence was examined using a Zeiss LSM confocal microscope (Thornwood, NY) with an xyz-motorized platform and Zeiss LSM software to obtain a z-stack.

### 2.16. Western blot

Prepared Caco-2 cells were lysed in RIPA buffer (Thermo Fisher Scientific) containing protease inhibitors. The proteins were separated using sodium dodecyl sulfate-polyacrylamide gel electrophoresis and then electroblotted onto polyvinylidene fluoride membranes. The membranes were blocked for 1 h at room temperature in 5% skim milk and then incubated with primary antibodies. After incubation with secondary antibodies, peroxidase activity was visualized on film using a chemiluminescence reagent.

### 2.17. Statistical analysis

Data were analyzed using GraphPad Prism software, and all summary data are presented as mean± standard error of the mean values. The statistical significance of differences was evaluated using the Student's t-test or one-way analysis of variance with Tukey's multiple comparison test. A P-value less than 0.05 was considered statistically significant.

### 2.18. Ethic statement

All animal care was performed according to the Guide for the Care and Use of Laboratory Animals of the Institute of Laboratory Animal Resources. All animal experiments were approved by the Animal Investigation Committee of KIRAMS (kirams 2020-0025; 2020-0069).

### 2.19. Role of funding source

Funders provided financial support for this study, but did not participate in the study design, data analyses, interpretation, or writing of the paper.

## 3. Results

### 3.1. Pravastatin mitigates acute radiation-induced enteropathy in a minipig model

To evaluate the therapeutic effects of PS on progression of radiation-induced enteropathy, we established a radiation-induced GI injury model by exposing abdomens of minipigs to radiation (Supplementary Fig. 1a). The minipig is a large animal used as a model in the

field of laboratory animal medicine; its GI tract anatomy and physiology are similar to humans [29]. The minipig is a useful animal model for evaluating radiation-induced GI damage because clinical symptoms after radiation exposure are similar to humans [30]. Minipigs had severe clinical symptoms, such as watery stool, decreased movement, and appetite loss after radiation exposure (Fig. 1a). At 2 weeks after radiation exposure, we identified irradiation-associated hemorrhagic and congestive changes in the small and large intestines (Fig. 1b). CRP is a marker of acute systemic inflammation. Irradiated minipigs had elevated plasma CRP levels (Fig. 1c) and neutrophil infiltration in mucosal and submucosal lesions (Supplementary Fig. 1b). We also found increased mRNA levels of (pro-) inflammatory cytokines, such as interleukin *(IL)-1b, IL-6*, and *MCP-1* in intestinal tissue (Supplementary Fig. 1c). Histological analysis revealed that irradiated small and large intestinal tissue had vascular enlargement, hemorrhage, and destruction of crypts and epithelium (Fig. 1d). Tissues of the small intestines had severe histological damage with loss of goblet cells and epithelial continuity (Fig. 1e). Alterations in plasma citrulline and endotoxin levels are associated with epithelial barrier damage and disruptions in intestinal permeability. The serological analysis revealed intestinal epithelial damage with endotoxemia in irradiated minipigs (Fig. 1f and 1g).

In previous studies using a mouse model, we found that PS had therapeutic effects in radiation-induced enteropathy [13,14]. In this study, we used PS for 2 weeks to treat minipigs that had local exposure to abdominal irradiation. The PS-treated irradiated animals had mild clinical symptoms (Fig. 1a) and alleviated pathological changes in the small and large intestines (Fig. 1b). We also found decreased plasma CRP levels (Fig. 1c) and inhibition of neutrophil accumulation with reduced inflammatory cytokine expression in the small intestines of the PS-treated irradiated minipigs (Supplementary Fig. 1b and 1c). The histological analysis revealed that PS-treated minipigs had many regenerative crypt structures and complete epithelial layers with goblet cells in the small and large intestines (Fig. 1d and 1e). Radiation-induced intestinal epithelial damage with accompanying endotoxemia was also relieved using PS treatment (Fig. 1f and 1g).

### 3.2. Pravastatin restores intercellular junctions in radiation-induced epithelial damage in a minipig model

To determine the therapeutic target of PS in radiation-induced enteropathy, we performed mRNA-seq using minipig small intestine tissue. First, we analyzed mRNA-seq data from the control (Con), irradiation (IR), and IR+PS groups using heat maps and one-way hierarchical cluster analysis. The analysis found transcriptomic differences of 6,688 genes, which were $|\log2 \text{ (fold-change)}| > 2$ between the Con and IR groups or the IR and IR+PS groups (Fig. 2a). These results indicated that radiation-induced gene alteration in the small intestine was normalized using PS treatment. The Con group and IR+PS group clustered more closely to each other than to the IR group, and the IR group was separated from the Con and IR+PS groups. Gene ontology enrichment analysis found significantly affected categories of genes associated with immune responses, inflammatory responses, oxidative reduction processes, regulation of cell proliferation, cell adhesion, regulation of apoptotic processes, angiogenesis, and cell migration (Fig. 2b). KEGG pathway analysis found that the MAPK signaling pathway, focal adhesion, cell adhesion molecules, and TJs were highly associated with PS treatment in the irradiated intestine (Fig. 2c). We also found significant differences in gene expression of cell adhesion markers, including TJ, AJ, and desmosome molecules between PS-treated irradiated intestinal tissue and irradiated intestinal tissue (Fig. 2d).

As mRNA-seq data indicated altered gene expression of intercellular junctions, we performed real-time RT-PCR and immunohistochemistry to identify characteristics of these changes in expression. The mRNA levels of *cadherin-1* (*CDH-1*) significantly increased in the PS-treated irradiated group compared with the IR group (Fig. 2e). Loss of apical E-Cad expression via irradiation was alleviated in the PS-treated animals (Fig. 2f). mRNA levels of TJ molecules (e.g., *ZO-1* and *OCLN*) and desmosome molecules (*DSG2)* also markedly decreased in irradiated minipigs, but PS treatment significantly improved these intercellular junction molecules (Fig. 2e). Immunohistochemistry analysis revealed that TJ proteins (ZO-1 and OCLN) and DSG2 had diminished expression in irradiated epithelium. PS treatment alleviated destruction of these TJ proteins and DSG2 expression (Fig. 2f). Therefore, PS mitigated radiation-induced enteropathy and enhanced intestinal epithelial barrier function via increases in intercellular junction molecules.

### 3.3. Larazotide acetate, a tight junction regulator, mitigates radiation-induced enteropathy

Radiation-induced epithelial barrier dysfunction and uncontrolled permeability associated with GI-ARS is well-known [2]. However, there is little known about whether reinforcement of the epithelial barrier is an effective therapeutic target for radiation-induced enteropathy. LA, an eight amino acid peptide, was the first in a novel class of drugs examined for TJ regulation during celiac disease treatment. The critical role of LA is to strengthen intestinal epithelial integrity and paracellular permeability [31,32]. To identify whether regulation of intercellular junctions alleviated radiation-induced enteropathy, we used LA as a treatment after local abdominal irradiation in a mouse model. Irradiated mice had severe body weight loss and bacterial translocation to mesenteric lymph nodes (Fig. 3a and 3b). We also found histological alterations consequent to radiation exposure. Irradiated intestines had crypt destruction, villus shortening, epithelial erosion, inflammatory cell infiltration in the mucosa and submucosa, and decreased epithelial proliferation (Fig. 3c-g). Histological scores that accounted for epithelial and crypt damage severity, vascular enlargement, and inflammation were also significantly increased in the IR group compared with the Con group (Fig. 3h). LA treatment in nonirradiated mice did not elicit any significant differences in ileum tissues compared with control mice (Supplementary Fig. 2a). Otherwise, LA treatment of irradiated mice increased mean body weight and inhibited bacterial translocation to the mesenteric lymph nodes (Fig. 3a and 3b). We also found significant declines in histological scores with increased villus lengths, crypt count, and epithelial proliferation in the LA-treated irradiated group compared with the IR group (Fig. 3c, 3d, and 3f-h). Immunostaining of villin revealed that LA treatment restored epithelial structures damaged by irradiation (Fig. 3e). The LA-treated group had decreased inflammatory cytokine expression and accumulation of monocytes and macrophages in intestinal tissue (Supplementary Fig. 2b, 2c, and 2e), but there was no significant difference in leucine-rich repeat-containing G-protein coupled receptor 5 levels, which is a marker of intestinal stem cells [33] (Supplementary Fig. 2d). Expression of intercellular junction molecules (e.g., E-Cad, Zo-1, Ocln, and Dsg2) was diminished in irradiated intestinal epithelium (Fig. 3i). The mRNA levels of intercellular junctions also significantly decreased in the IR group compared with the Con group (Fig. 3j). LA treatment restored localization and expression of intercellular junction molecule in irradiated mice (Fig. 3i). The mRNA levels of *Cdh-1, Zo-1, Ocln,* and *Dsg2* significantly increased in the LA-treated irradiated group compared with the IR group (Fig. 3j). We found that LA-treated mice resisted radiation-induced enteropathy by enhancing of the epithelial barrier. These results suggested that the epithelial intercellular junction is a novel therapeutic target for radiation-induced enteropathy.

### 3.4. Pravastatin regulates intercellular junctions and enhances epithelial integrity in irradiated Caco-2 monolayers

To examine whether PS directly affected intercellular junction molecules and epithelial integrity in vitro, we performed epithelial

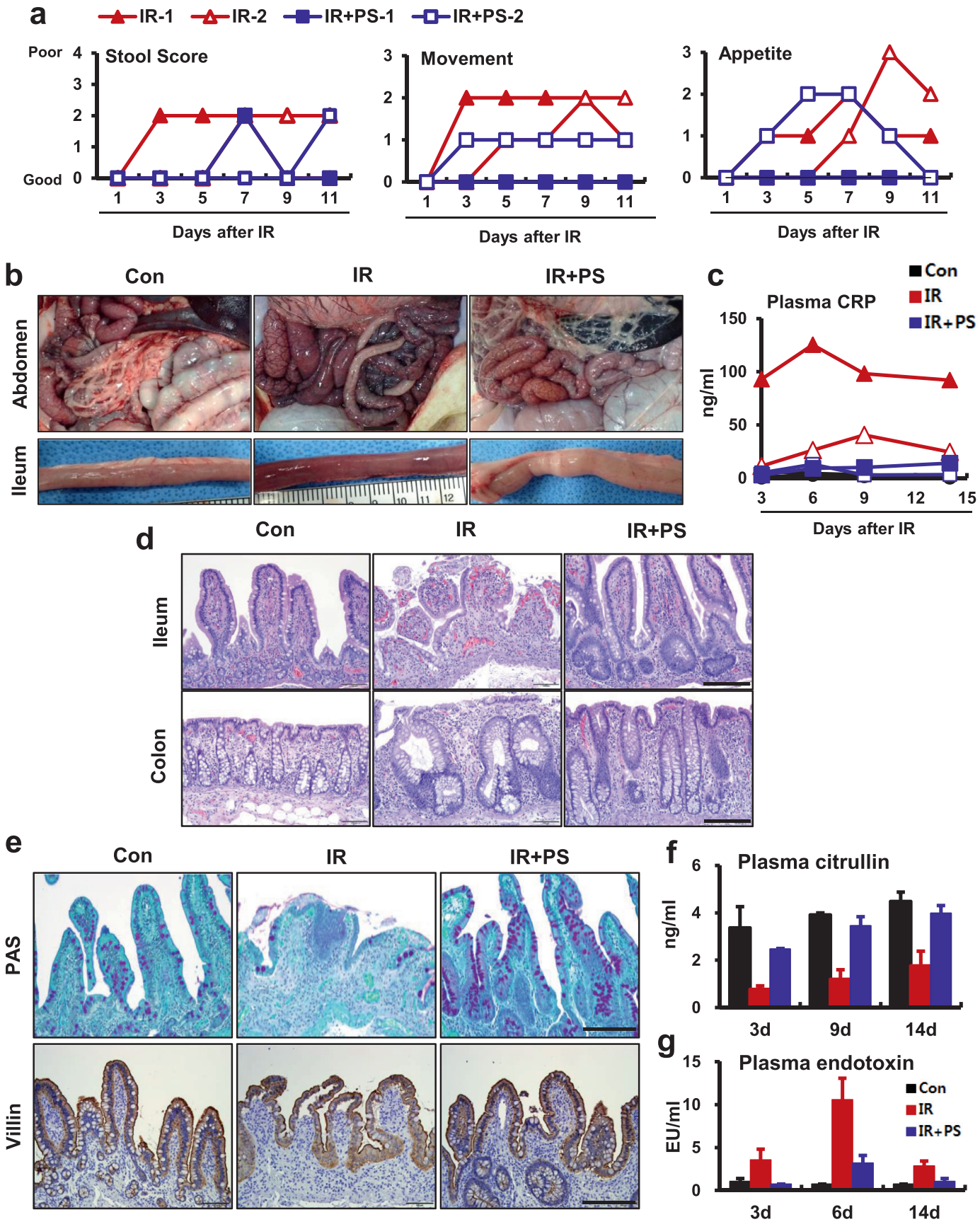


**Figure 1. Pravastatin attenuates acute radiation-induced enteropathy in a minipig model.** (a) Clinical scores including stool condition, movement, and appetite in irradiated (IR) and pravastatin-treated irradiated (IR+PS) minipigs. (b) Gross appearance of intestine in control (Con), IR, and IR+PS minipigs. (c) Plasma CRP levels in Con, IR, and IR+PS minipigs. (d) H&E-stained ileum and colon tissues. (e) Periodic acid-Schiff stain and immunohistochemistry of villin of the small intestine from Con, IR, and IR+PS groups 14 days after 15 Gy irradiation. Bar= 200 $\mu$m. (f) Citrulline and (g) endotoxin levels of plasma in Con, IR, and IR+PS minipigs. Results are presented as mean ± standard error of the mean values; n = 2 minipigs per group.

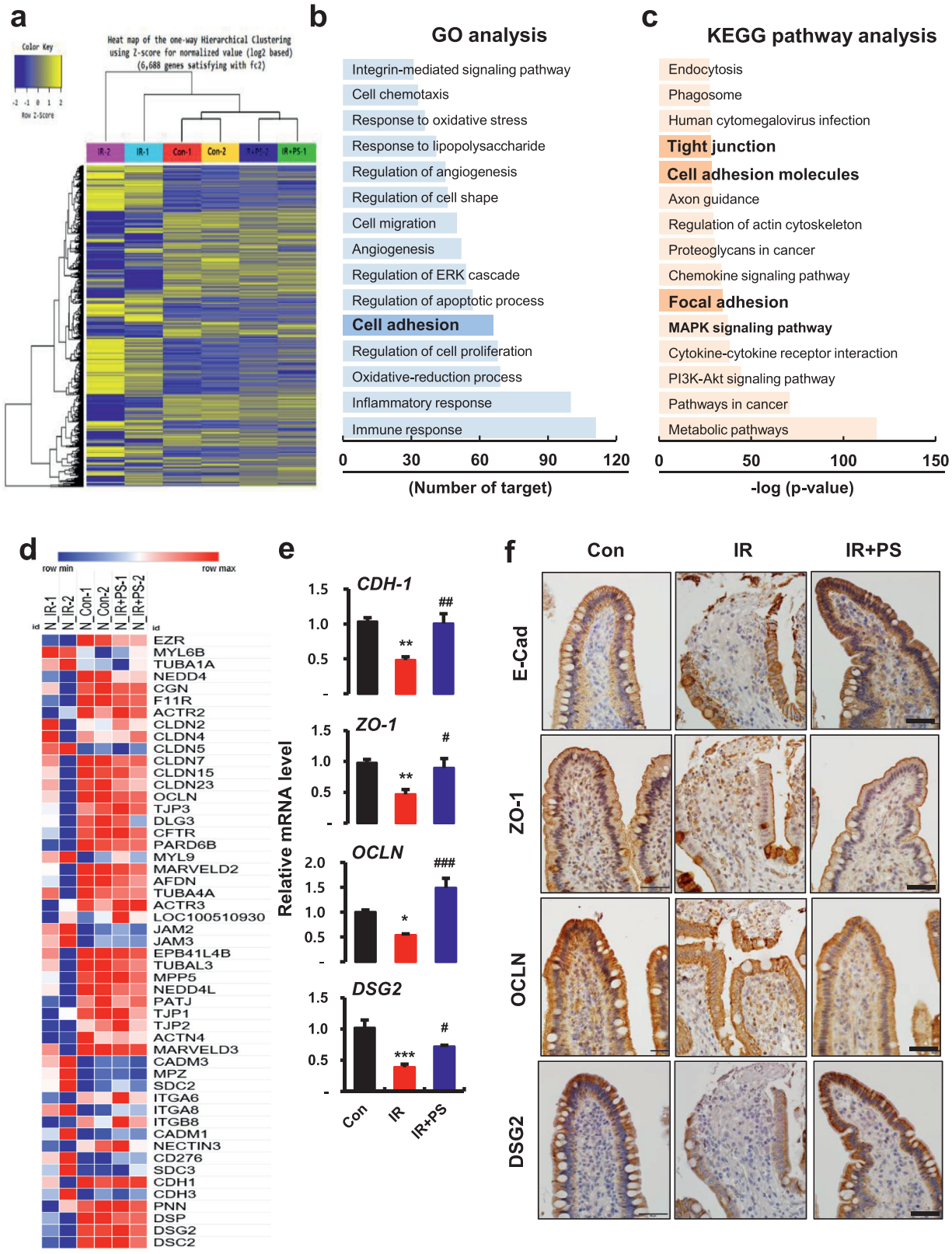


**Figure 2. Pravastatin restores radiation-damaged epithelial intercellular junctions.** (a) Heatmap of hierarchical clustering. Indication of differentially expressed genes (rows) between control (Con), irradiated (IR) and pravastatin-treated IR (IR+PS) groups (fold-change > 2, P < 0.05). Yellow indicates high relative gene expression. Blue indicates low relative gene expression. (b) Gene ontology (GO) and (c) Kyoto Encyclopedia of Genes and Genomes (KEGG) pathway analyses of differentially expressed genes. (d) Heatmap of intercellular junction-related genes. Red represents high relative gene expression. Blue represents low relative gene expression. n = 2 minipigs per group. (e) mRNA levels of *cadherin-1 (CDH-1), zonula occludens (ZO)-1, occludin (OCLN),* and *desmoglein 2 (DSG2),* and immunoreactivity of (f) E-cadherin (E-Cad), ZO-1, OCLN, and DSG2 in ileum tissue from Con, IR, and IR+PS minipigs. Bar = 50 $\mu$m. n = 4 small intestinal tissue pieces from each group. One-way ANOVA was used to compare the results. Results are presented as mean ± standard error of the mean values. $^{*}P < 0.05$, $^{**}P < 0.01$, $^{***}P < 0.001$ compared to control group; $^{\#}P < 0.05$, $^{\#\#}P < 0.01$, $^{\#\#\#}P < 0.001$ compared to IR group.

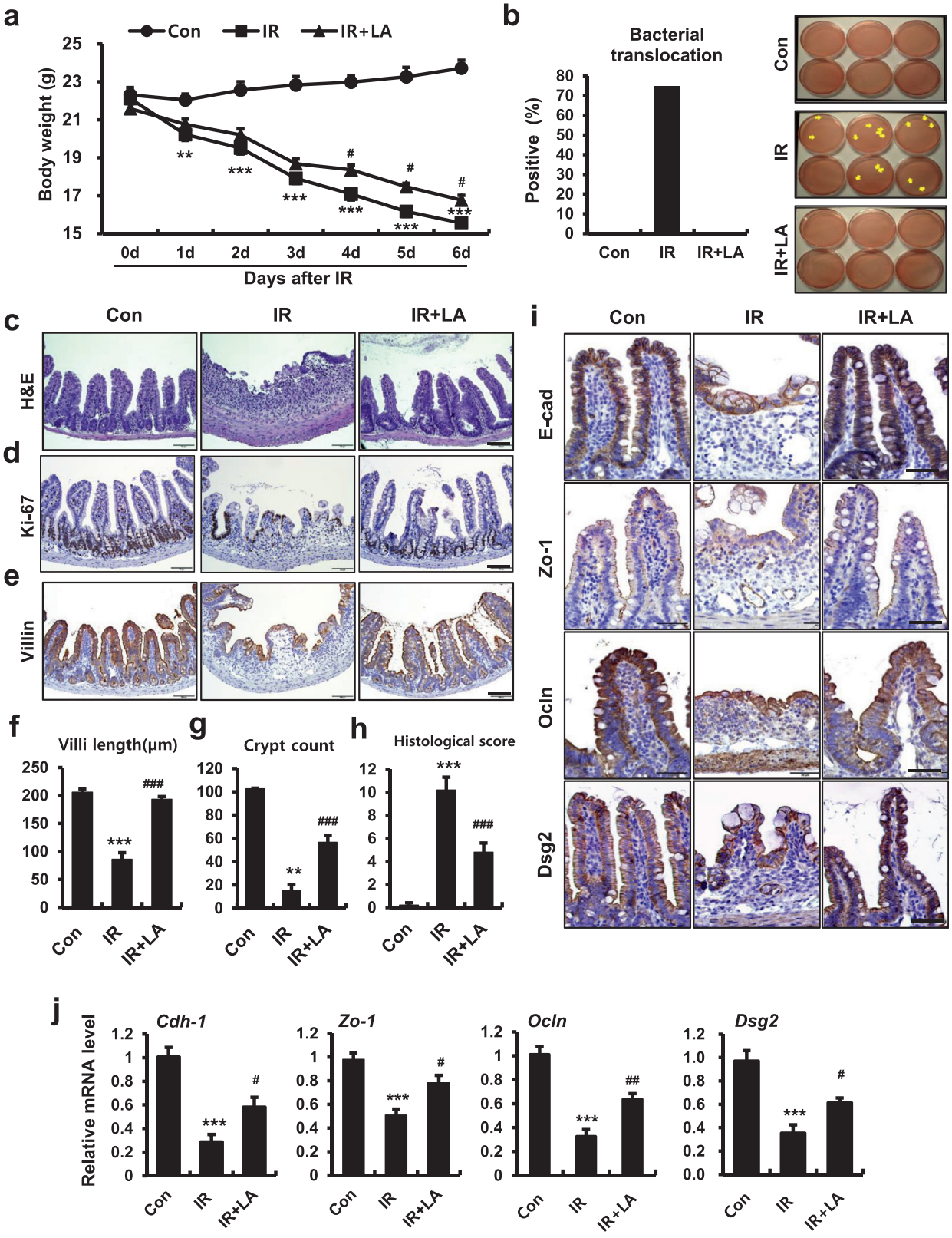


**Figure 3. The tight junction regulator, larazotide acetate, alleviates radiation-induced enteropathy in a mouse model.** (a) Measurement of body weight for 6 days in control (Con), irradiated (IR), and larazotide acetate-treated IR (IR+LA) mice. (b) Bacterial translocation assay of mesenteric lymph nodes, (c) H&E staining and immunoreactivity of (d) Ki-67 and (e) villin in small intestines of Con, IR, and IR+PS groups. Bar = 100 $\mu$m. (f) Villus lengths, (g) crypt numbers in the circle, and (h) histological scores for small intestines from Con, IR, and IR+PS groups. (i) Immunoreactivity and (j) mRNA levels of *Cdh-1, Zo-1, Ocln*, and *Dsg2* in ileum tissue of Con, IR, and IR+LA mice. Bar = 50 $\mu$m. One-way ANOVA was used to compare the results. Results are presented as mean ± standard error of the mean values; n = 6-7 mice per group. $^{**}P < 0.01$, $^{***}P < 0.001$ compared to control group; $^{\#}P < 0.05$, $^{\#\#}P < 0.01$, $^{\#\#\#}P < 0.001$ compared to IR group. All data represent at least two independent experiments.

functional analysis using a Caco-2 monolayer system. This model is widely used to study the human intestinal barrier [27,28]. First, we measured epithelial paracellular permeability using TEER and 4-kDa FITC-dextran assay [34]. Irradiated Caco-2 monolayers had uncontrolled permeability consistent with decreased TEER levels and increased FITC concentrations in the culture medium of the lower chamber (Fig. 4a and 4b). Dispase-based dissociation assay results indicated the adhesive force of the epithelial cells was dependent on the AJs and desmosomes, and these attachments were fragile in irradiated epithelial cells (Fig. 4c). In contrast, PS treatment significantly attenuated paracellular permeability in radiation-induced epithelial damage (Fig. 4a and 4b). Dispase-based dissociation assay found that PS treatment enhanced epithelial attachment in irradiated conditions (Fig. 4c). Confocal analysis revealed that radiation exposure changed the localization of E-Cad in Caco-2 monolayers (Fig. 4d). While PS treatment partially restored E-Cad localization (Fig. 4d), there was no alteration in mean levels of protein expression in irradiated Caco-2 monolayers (data not shown). We also found that radiation exposure resulted in destruction of intercellular junctions (e.g., ZO-1, OCLN, and DSG2) and in declines in protein and mRNA expression of these molecules in Caco-2 monolayers (Fig. 4d-f). PS treatment restored losses of intercellular junction molecules and increased protein and mRNA levels of *ZO-1, OCLN, DSG2* in irradiated Caco-2 monolayers (Fig. 4d-f). Activation of p38 MAPK leads to the downregulation of intercellular junctions, including OCLN, ZO-1, and DSG2, contributing to the increase in epithelial permeability [35,36]. We also found that PS inhibited the phosphorylation of p38 MAPK in irradiated Caco-2 monolayers (Fig. 4g). These results indicated that PS improved epithelial integrity by regulating intercellular junction molecules and inhibiting p38 MAPK in radiation-induced epithelial damage.

### 3.5. Pravastatin upregulates metallothionein 1 and 2 in irradiated epithelial cells

To examine how PS regulated intercellular junction molecules in irradiated epithelial cells, we used mRNA-seq to analyze target molecules of PS in irradiated intestine. We compiled the representative top 50 most significant genes with altered expression downregulated by irradiation and upregulated by PS treatment. In these 50 genes, MT1 subtype genes (MT1E: ranked 5, MT1A: ranked 7) and MT2 genes (ranked 50) ranked high in gene alteration. We also found that MT1/2 were expressed in the intestinal epithelium and this expression was decreased in irradiated minipig intestines (Fig. 5a). mRNA levels of *MT1A, MT1E,* and *MT2* were also significantly decreased in these tissues (Fig. 5b). In contrast, PS treatment increased MT1/2 expression in the epithelium of irradiated intestines (Fig. 5a). mRNA levels of MT1A, MT1E, and MT2 were significantly increased in PS-treated irradiated minipigs compared with untreated irradiated minipigs (Fig. 5b). Using immunofluorescence and western blot analysis, we also identified decreased expression of MT1/2 protein under irradiation in the Caco-2 monolayers (Fig. 5c and 5d). The levels of MT1A, MT1E, and MT2 genes also decreased in the IR group compared with the Con group (Fig. 5e). In contrast, PS-treated irradiated Caco-2 monolayers had upregulation of MT1/2 protein expression (Fig. 5c and 5d). mRNA levels of *MT1A, MT1E*, and *MT2* also significantly increased in the PS-treated irradiated group compared with the IR group (Fig. 5e). Taken together, these results indicated that PS increased epithelial MT1/2 expression in irradiated intestinal epithelium.

### 3.6. Metallothionein 1 and 2 enhance intercellular junctions and improve epithelial integrity in irradiated Caco-2 monolayers

Exogenous MT1/2 rapidly internalizes in the cytosol of epithelial cells of intestine and kidney, neurons, and astrocytes of the central nervous system [37-39]. We also identified increased cellular MT1/2 levels in exogenous MT1- or MT2-treated Caco-2 monolayer systems (Supplementary Fig. 3). To determine whether MT1/2 affected epithelial integrity and intercellular junction molecules, like PS in irradiated epithelial cells, we examined epithelial functional assays using treatment with exogenous MT1 or MT2. MT1 or MT2 treatment attenuated epithelial barrier damage and paracellular permeability in irradiated Caco-2 monolayers (Fig. 6a and 6b). The dispase-based dissociation assays revealed that MT1 or MT2 treatment enhanced epithelial attachment in the irradiated condition (Fig. 6c). The combination of MT1 and MT2 did not improve paracellular permeability and resistance to dispase, compared with MT2-treated irradiated Caco-2 monolayers (data not shown). Confocal analysis found that MT1 or MT2 treatment improved intercellular junction (ZO-1, OCLN, and DSG2) disturbance associated with radiation exposure (Fig. 6d). Intercellular junction protein levels markedly increased in MT1- or MT2-treated irradiated Caco-2 monolayers, compared with untreated irradiated Caco-2 monolayers (Fig. 6f). MT2 treatment more effectively upregulated intercellular junction expression than MT1 treatment. The results for mRNA expression indicated that while MT1 treatment significantly increased *DSG2* levels, MT2 treatment increased *ZO-1, OCLN*, and *DSG2* levels, in the irradiated Caco-2 monolayers (Figure 6g). We also found that MT2 treatment inhibited the phosphorylation of p38 MAPK in irradiated Coco-2 monolayers (Fig. 6e). Taken together, these results indicated that MT1 and MT2 enhanced epithelial integrity by regulating intercellular junction molecules. MT2 regulated intercellular junctions and p38 MAPK inactivation more effectively than MT1 in irradiated Caco-2 monolayers.

### 3.7. Pravastatin increases intercellular junction formation and reinforces epithelial integrity by regulating metallothionein 2

Next, we altered MT2 expression in human intestinal epithelial cells using small interfering RNA (siRNA)-mediated gene silencing to examine the role of MT2 in PS-related epithelial junction formation and cell permeability in Caco-2 monolayers. First, we found that mRNA and protein levels of MT2 markedly decreased in siRNA targeting MT2 (si-MT2)-treated Caco-2 cells; other MT subtype genes, such as MT1A and MT1E, did not change (Fig. 7a and 7b). si-MT2 alone treated Caco-2 monolayers had slightly decreased TEER levels and increased FITC concentrations in the culture medium, compared with those of the Con group (Fig. 7c and 7d). The dispase-based dissociation assay revealed that MT2 deficiency partially induced fragile attachment in Caco-2 monolayers (Fig. 7e). While PS treatment markedly improved epithelial permeability and attachment in irradiated Caco-2 monolayers, PS treatment in MT2-deficienct Caco-2 monolayers did not restore TEER levels, FITC levels, or attachment degree (Fig. 7c-e). Using confocal analysis we found that si-MT2 alone treatment resulted in loss of connection of intercellular junctions, and that protein and mRNA levels of OCLN and DSG2 were decreased (Fig. 8a-c). While PS treatment recovered the losses of intercellular junctions in irradiated Caco-2 monolayers, there were no improvements in the localization and expression of these junctions under MT2-deficient conditions (Fig. 8a-c). In addition, PS treatment of MT2-deficienct Caco-2 monolayers did not inhibit phosphorylation of p38 MAPK under irradiation conditions (Fig. 8d). Taken together, these results indicated that PS enhanced intercellular junctions with epithelial integrity via MT2 under irradiation conditions.

### 3.8. Metallothionein 2 alleviates radiation-induced enteropathy by regulating epithelial barrier function

To investigate whether MT2 could be a therapeutic target for radiation-induced enteropathy, we applied MT2 (10 $\mu$g/day) after abdominal irradiation of mice. MT2 treatment of nonirradiated mice did not show any significant difference in ileum tissues compared with control mice (Supplementary Fig. 4a). MT2 treatment of

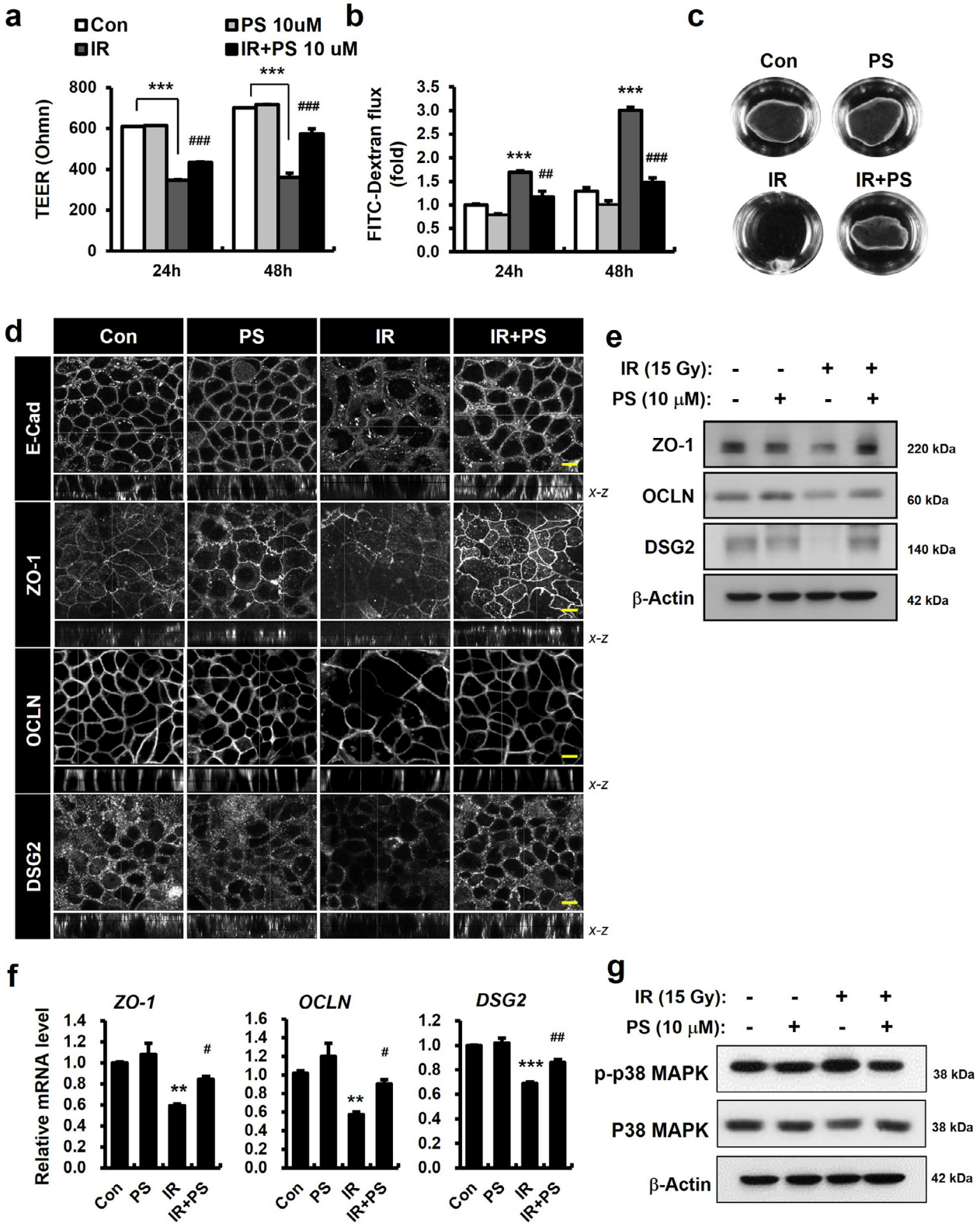


**Figure 4. Pravastatin regulates intercellular junctions and improves epithelial integrity.** (a) Transepithelial electrical resistance (TEER), (b) FITC-dextran, and (c) dispase-based dissociation assay in control (Con), pravastatin (PS)-treated, irradiated (IR), and IR+PS-treated Caco-2 monolayers. (d) Immunofluorescence of E-Cad, ZO-1, OCLN, and DSG2 in Con, PS, IR, and IR+PS-treated Caco-2 monolayers. (e) Western blot analysis and (f) mRNA levels of *ZO-1*, *OCLN*, and *DSG2*. (g) Western blot analysis of phosphorylated p38 MAPK (p-p38 MAPK) and toral p38 MAPK (p38 MAPK) in Con, PS, IR, and IR+PS-treated Caco-2 monolayers. Bar = 10 $\mu$m. One-way ANOVA was used to compare the results. Results are presented as mean ± standard error of the mean values; n = 3-4 per group. $^{**}P < 0.01$, $^{***}P < 0.001$ compared to control group; $^{\#}P < 0.05$, $^{\#\#}P < 0.01$, $^{\#\#\#}P < 0.001$ compared to IR group. All data represent at least two independent experiments.text=

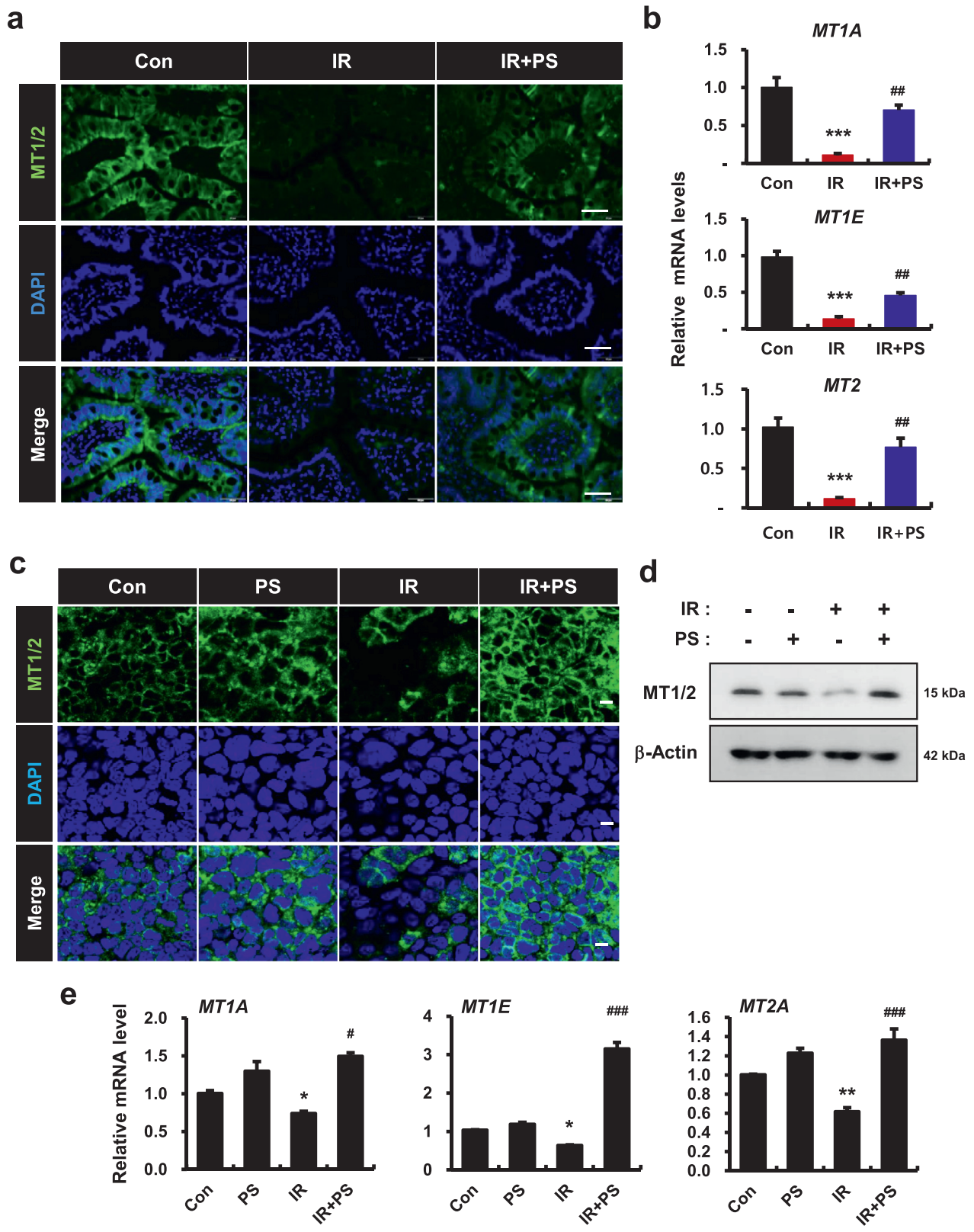


**Figure 5. Pravastatin regulates metallothionein 1 and 2 expression in irradiated epithelial cells.** (a) Immunoreactivity of metallothionein (MT) 1/2 in in the small intestine of control (Con), irradiated (IR), and pravastatin-treated IR (IR+PS) minipigs. Bar = 50 $\mu$m. (b) mRNA levels of *MT1A, MT1E*, and *MT2* in Con, IR, and IR+PS minipigs. (c) Immunofluorescence of MT1/2 in Con, PS, IR, and IR+PS treated Caco-2 monolayers. Bar = 10 $\mu$m. (d) Protein expression of MT1/2 and (e) mRNA levels of *MT1A, MT1E*, and *MT2* in Con, PS, IR, and IR +PS-treated Caco-2 monolayers. One-way ANOVA was used to compare the results. Results are presented as mean ± standard error of the mean values; n = 3-4 per group. $^{*}P < 0.05$, $^{**}P < 0.01$, $^{***}P < 0.001$ compared to control group; $^{\#}P < 0.05$, $^{\#\#}P < 0.01$, $^{\#\#\#}P < 0.001$ compared to IR group. All data represent at least two independent experiments.

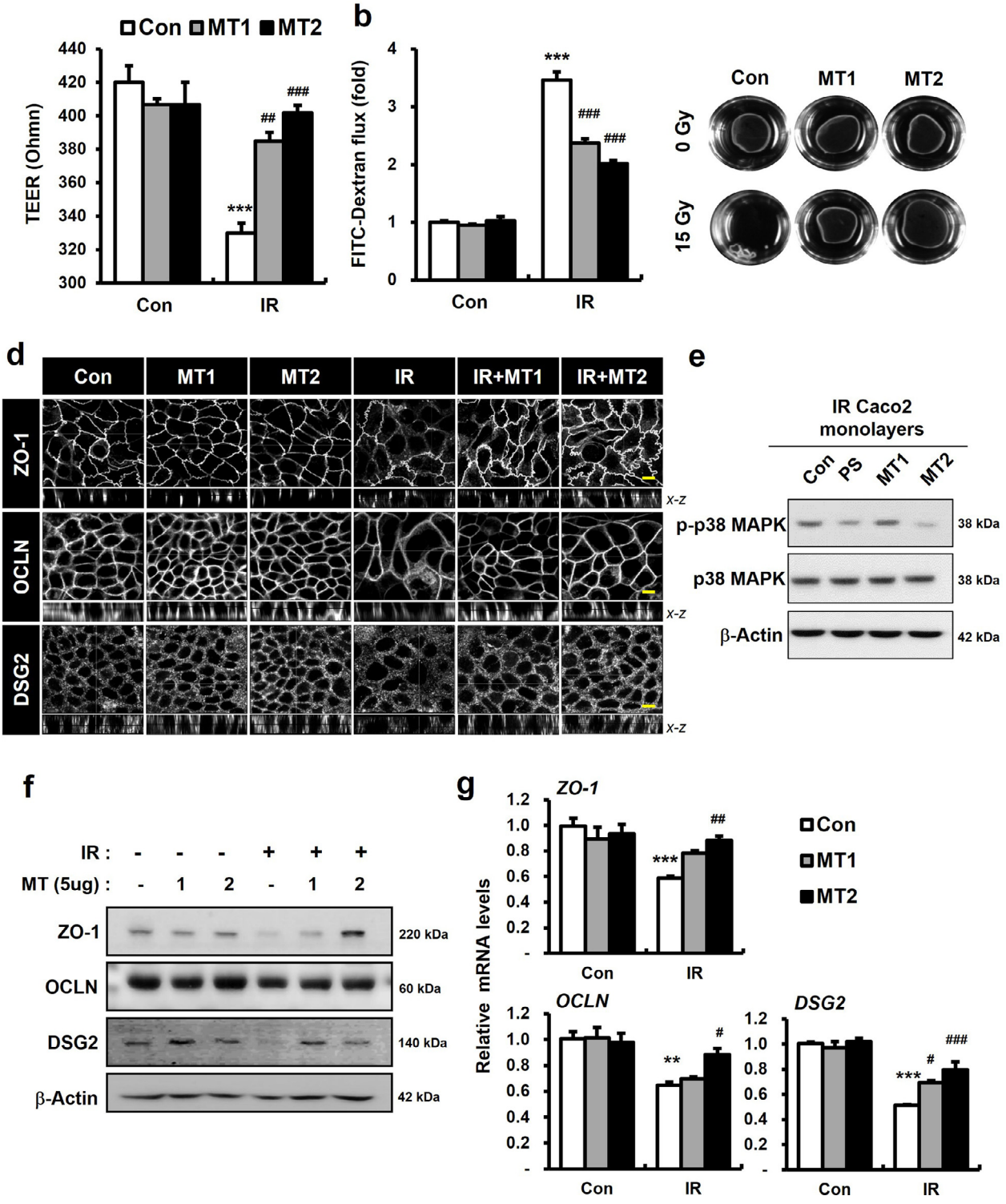


**Figure 6. Metallothionein 1 and 2 regulate intercellular junctions in radiation-induced epithelial damage.** (a) TEER, (b) FITC-dextran, and (c) dispase assay in control (Con), metallothionein (MT)1, and MT2 with/without irradiation (IR) treatment in Caco-2 monolayers. (d) Immunofluorescence of ZO-1, OCLN, and DSG2 in Con, MT1, and MT2 with/without irradiation (IR) treatment in Caco-2 monolayers. Bar= 10 $\mu$m. (e) Western blot analysis of phosphorylated p38 MAPK (p-p38 MAPK) and toral p38 MAPK (p38 MAPK) in Con, PS, MT1, and MT2-treated irradiated Caco-2 monolayers. (f) Western blot analysis and (g) mRNA levels of *ZO-1*, *OCLN*, and *DSG2* in Con, MT1, and MT2 with/without IR treatment in Caco-2 monolayers. One-way ANOVA was used to compare the results. Results are presented as mean ± standard error of the mean values; n = 3-4 per group. $^{**}P < 0.01$, $^{***}P < 0.001$ compared to control group; $^{\#}P < 0.05$, $^{\#\#}P < 0.01$, $^{\#\#\#}P < 0.001$ compared to IR group. All data represent at least two independent experiments.text=

irradiated mice increased body weight and inhibited bacterial translocation to mesenteric lymph nodes (Fig. 9a and 9b). We also found that MT2 treatment significantly attenuated histological scores, and increased villus lengths, crypt numbers, and epithelial proliferation, compared with the IR group (Fig. 9c, 9d, and 9f-h). The MT2-treated group had an inhibited inflammatory response with decreased inflammatory cytokine expression, such as Il-6, Mcp-1, and monocyte and macrophage accumulation in mucosal and submucosal tissue (Supplementary Fig. 4b, 4c, and 4e), and improvements in intestinal stem cell properties in irradiated intestine (Supplementary Fig. 4d).

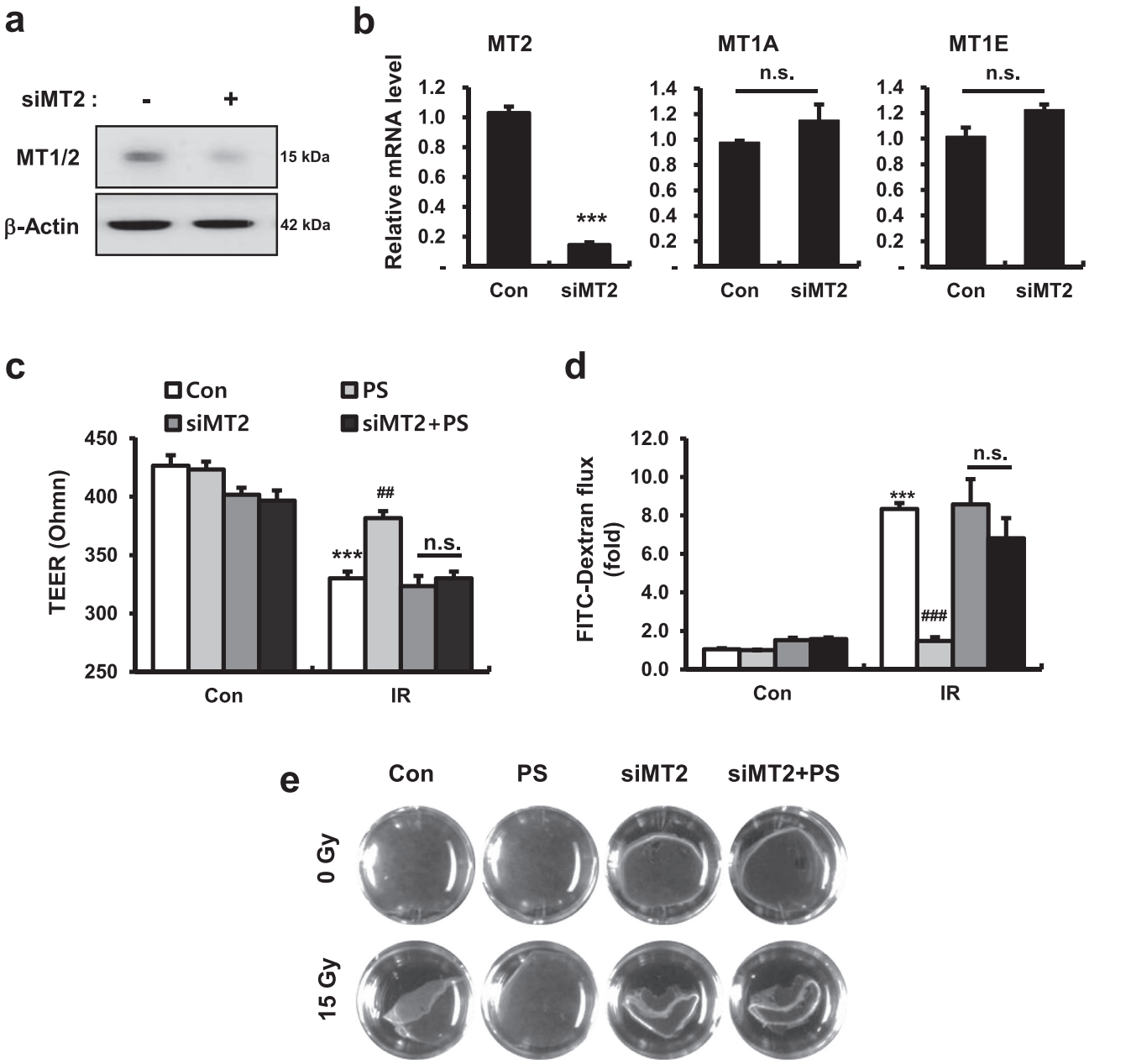


**Figure 7. Pravastatin does not reinforce epithelial integrity in metallothionein 2-deficient conditions.** (a) Protein expression of metallothionein (MT) 1/2 and (b) mRNA levels of *MT2, MT1A,* and *MT1E* in si-MT2-treated Caco-2 monolayers. The student's *t*-test was used to compare the results. n.s., not significant; $^{***}P < 0.001$ compared to the control group (c) TEER, (d) FITC-dextran, and (e) dispase-based dissociation assay in control (Con), pravastatin (PS), si-MT2, and si-MT2+PS with/without irradiation (IR) treatment in Caco-2 monolayers. One-way ANOVA was used to compare the results. Results are presented as mean ± standard error of the mean values; n = 3-4 per group. n.s., not significant; $^{***}P < 0.001$ compared to control group; $^{##}P < 0.01$, $^{###}P < 0.001$ compared to IR group. All data represent at least two independent experiments.

The immunostaining results indicated that MT2 treatment restored damaged intercellular junctions in irradiated mice (Fig. 9i). mRNA levels of *Cdh-1, Zo-1, Ocln,* and *Dsg2* significantly increased in the MT2-treated irradiated group, compared with the IR group (Fig. 9j). Taken together, these results indicated that in the MT2-treated mice, regulation of epithelial integrity alleviated radiation-induced intestinal injury.

## 4. Discussion

Use of minipig models before human clinical trials are performed has increased in recent years [40]. A major benefit of these models is the similarity between the swine GI tract anatomy and physiology and that of humans (e.g., transit time, pH value, and microbiota). The minipig is a suitable model for evaluation of pharmaceutical oral bioavailability [29]. It is a potentially more useful animal model than the rodent model for evaluating radiation-induced GI damage because the clinical symptoms of radiation damage (e.g., fever, vomiting, diarrhea) are similar to those of humans, and severe cases can result in death of the irradiated subject [30]. Therefore, the minipig model is a good alternative animal model for clinical therapeutic studies of radiation-induced enteropathy [30].

In this minipig model study, we found therapeutic effects of PS used for radiation-induced enteropathy. Abdominally irradiated minipigs had severe clinical symptoms, systemic inflammation, and endotoxemia with histopathological GI damage. The anti-inflammatory and anti-fibrotic therapeutic effects of PS for radiation-induced GI damage have been revealed using rodent models [14-16]. We

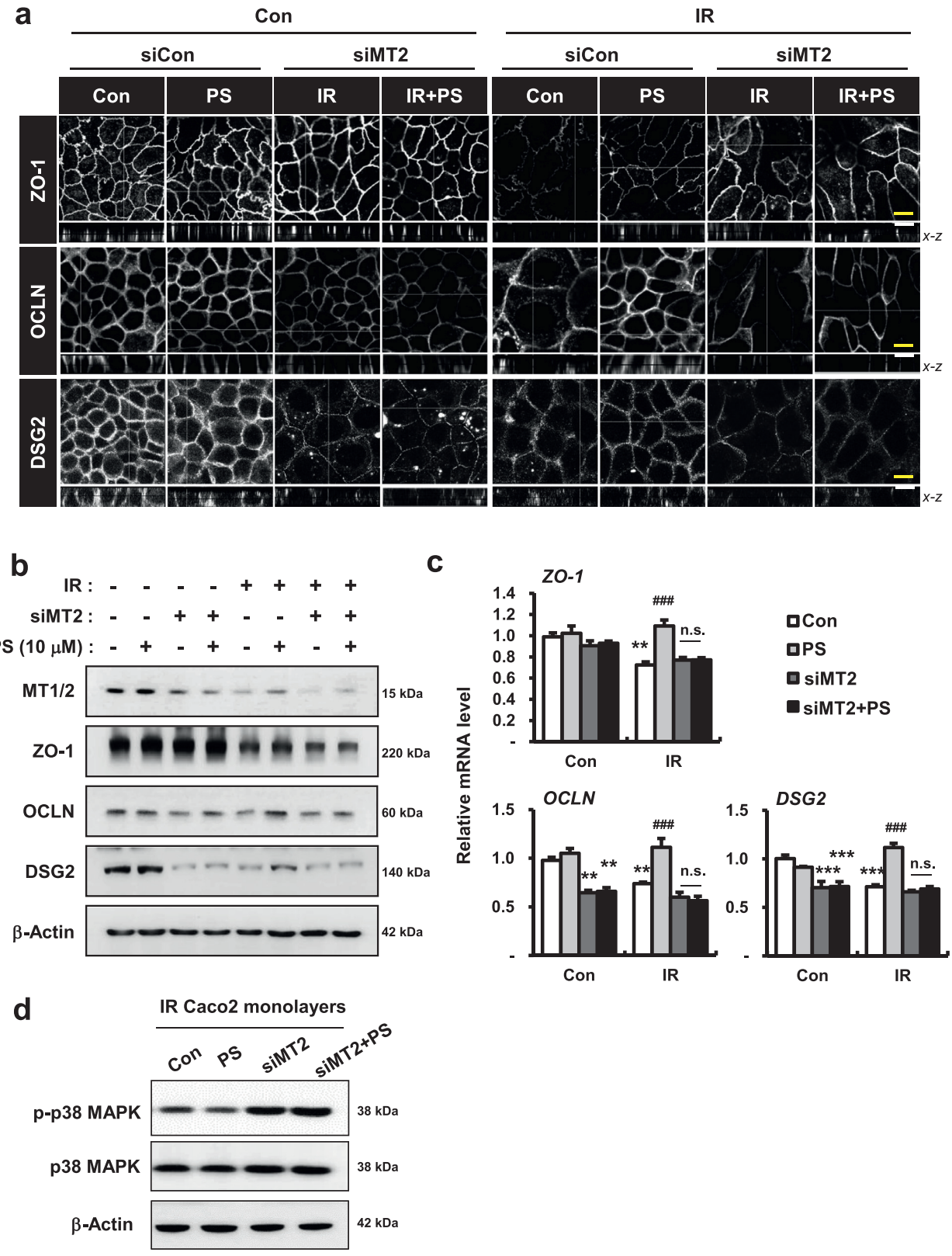


**Figure 8. Pravastatin attenuates radiation-induced intercellular junction damage by activating metallothionein 2.** (a) Immunofluorescence of ZO-1, OCLN, and DSG2 in control (Con), pravastatin (PS), si-MT2, and si-MT2+PS with/without irradiation (IR) treatment in Caco-2 monolayers. Bar = 10 $\mu$m. (b) Western blot analysis and (c) mRNA levels of *ZO-1*, *OCLN*, and *DSG2* in Con, PS, si-MT2, and si-MT2+PS with/without IR treatment in Caco-2 monolayers. (d) Western blot analysis of phosphorylated p38 MAPK (p-p38 MAPK) and total p38 MAPK (p38 MAPK) in Con, PS, si-MT2, and si-MT2+PS-treated irradiated Caco-2 monolayers. One-way ANOVA was used to compare the results. Results are presented as mean ± standard error of the mean values; n = 3-4 per group. n.s., not significant; $^{**}P < 0.01$, $^{***}P < 0.001$ compared to control group; $^{\#\#\#}P < 0.001$ compared to IR group. All data represent at least two independent experiments.

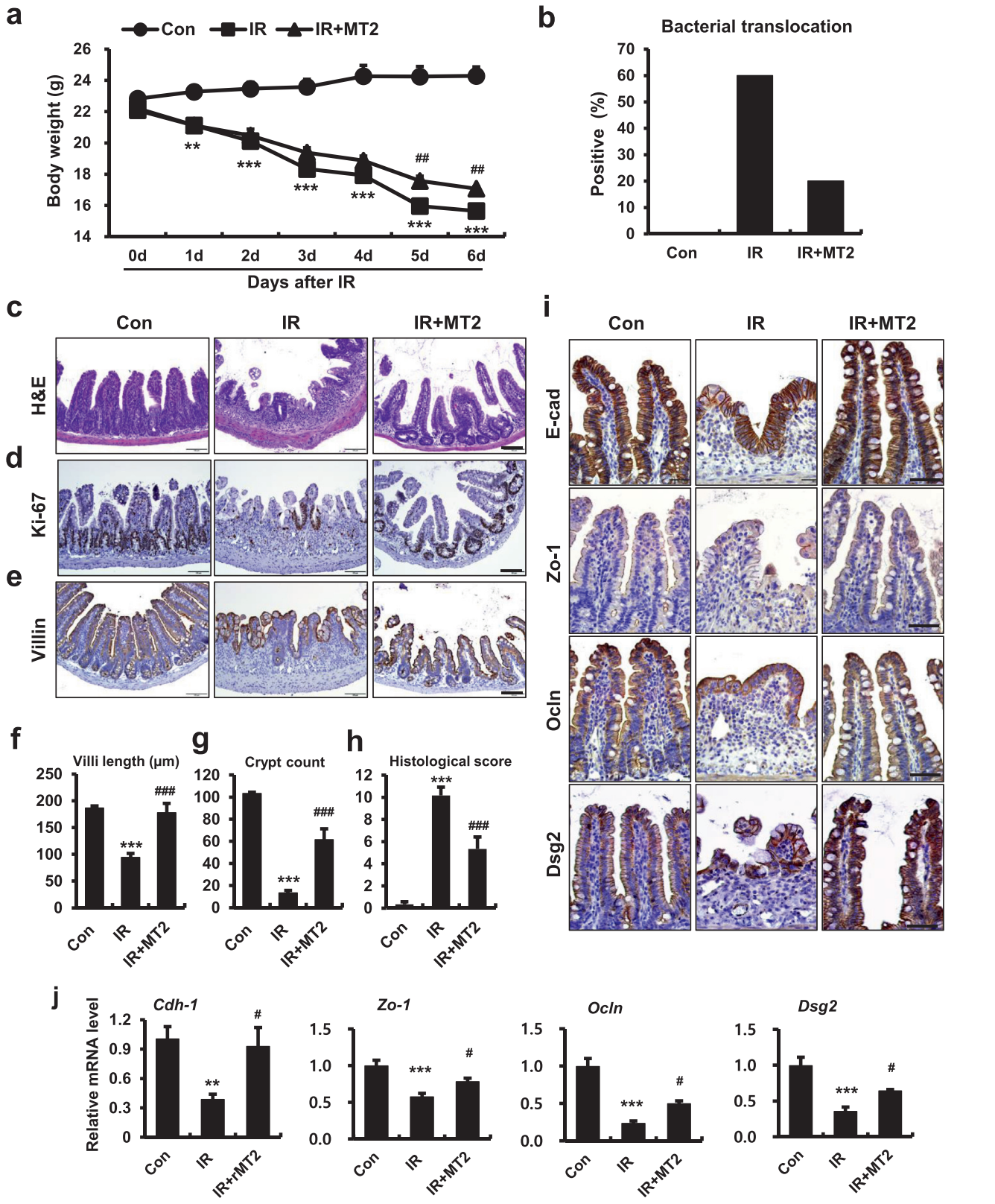


**Figure 9. Metallothionein 2 mitigates radiation-induced enteropathy with enhancement of intercellular junctions in a mouse model.** (a) Measurement of body weight for 6 days in control (Con), irradiated (IR), and metallothionein 2 (MT2)-treated IR (IR+MT2) mice. (b) Bacterial translocation assay in mesenteric lymph nodes, (c) H&E stain, and immunoreactivity of (d) ki-67 and (e) villin in small intestines of Con, IR, and IR+MT2 group mice. Bar = 100 $\mu$m. (f) Villus lengths, (g) crypt numbers in the circle, and (h) histological scores for small intestines in Con, IR, and IR+MT2 groups. (i) Immunoreactivity and (j) mRNA levels of *Cdh-1, Zo-1, Ocln,* and *Dsg2* in ileum tissue of Con, IR, and IR+MT2 treated mice. Bar = 50 $\mu$m. One-way ANOVA was used to compare the results. Results are presented as mean ± standard error of the mean values; n = 6 mice per group. $^{**}P < 0.01$, $^{***}P < 0.001$ compared to control group; $^{\#}P < 0.05$, $^{\#\#\#}P < 0.001$ compared to IR group. All data represent at least two independent experiments

found that oral PS treatment attenuated radiation-induced enteropathy and relieved clinical symptoms and the inflammation response in minipigs. To find the novel molecular target and active mechanism for PS treatment, we performed mRNA-seq analysis using ileum tissue from minipigs exposed to radiation. Using gene ontology and KEGG analysis, we found that PS application to irradiated intestinal tissue frequently affected immune and inflammatory responses and the extent of endothelial damage PS is known to reduce radiation-induced vascular damage of tissues [14]. Protection of vascular damage could affect epithelial function [41]. However, in this study, we focused on the direct effects of PS in irradiated epithelial cells. Cell adhesion- and TJ-related molecules were also markedly involved in the response of PS-treated irradiated intestine. Wilkinson et al. found that statin enhances TJ formation and prevents increased permeability in doxorubicin-induced endothelial toxicity [42]. We also found that epithelial intercellular junction proteins, including E-Cad, ZO-1, ZO-2, OCLN, and DSG2, improved when PS treatment was used in the irradiated minipigs. These results indicated that PS enhanced the intercellular junctions in the irradiated epithelium and mitigated radiation-induced enteropathy.

Intercellular junctions are crucial components of the epithelial barrier; TJs, AJs, and desmosomes form the apical junctional complex [43]. The TJ is the primary determinant of paracellular permeability. AJs and desmosomes provide adhesive forces necessary to maintain cell-cell interactions. DSG2 is a main molecule for maintenance of intestinal epithelial barrier functions by regulating adhesion in desmosomes [28]. Maintenance of this barrier has a pivotal role in protection of the organism against luminal pathogens. Increased paracellular permeability results in systemic contamination and potentially results in severe systemic inflammation [44,45]. Intercellular junction damage is a critical component of the etiologies of intestinal disorders, such as IBD, celiac disease, and infectious gastroenteritis [46,47]. Epithelial barrier dysfunction with intercellular junction loss is well-known in radiation-induced intestinal toxicity [11]. Otherwise, there are limited studies of intercellular junctions and epithelial barriers as therapeutic targets in radiation toxicity. In this study, TJ regulator (LA)-treated mice had reinforced intestinal permeability and intercellular junctions, and alleviation of histological damage induced by radiation exposure. These results suggested that maintenance and restoration of intercellular junction and epithelial integrity could be a therapeutic target for radiation-induced enteropathy.

It is known that p38 MAPK plays a role in the regulation of intercellular junctions including OCLN, ZO-1, and DSG2, contributing to the increase in epithelial permeability in response to various stimuli [35,36]. Using mRNA-seq analysis, MAPK signaling was shown to be critically involved in the therapeutic effects of PS in the minipig model of radiation-induced enteropathy. We used a Caco-2 monolayer system to examine whether PS directly affected functions associated with intestinal epithelial integrity and expression of intercellular junctions. Radiation exposure induced functional destruction of epithelial integrity and decreased expression of intercellular junctions and p38 MAPK activation in epithelial cells. In contrast, PS induced enhancement of epithelial integrity and expression of junction molecules and suppression of the phosphorylation of p38 MAPK in irradiated Caco-2 monolayers. These results indicated that PS improved epithelial integrity by regulating intercellular junction proteins, including ZO-1, OCLN, and DSG2, and inhibiting p38 MAPK in radiation-exposed epithelial cells.

MT1/2 have multiple functions, including detoxification of heavy metals and reduction of oxidative stress [19,20] and suppression of p38 MAPK activation [48,49]. We found that while MT1/2 expression decreased in irradiation conditions, MT1/2 markedly increased in the intestinal epithelium of PS-treated irradiated minipigs and in PS-treated irradiated Caco-2 monolayers. MT1/2 have protective effects in various disease models, including lipopolysaccharide-induced lung injury [50], rheumatoid arthritis [51], multiple sclerosis [52], coagulatory disturbances [24], and gastroenteritis [53,54]. MT1/2 also have an important role in protection of intestinal mucosa. MT1/2-deficient mice have more severe mucosal inflammation with epithelial destruction in dextran sodium sulfate-induced colitis and *Helicobacter pylori*-induced gastritis [53,54]. In IBD patients, MT1/2 concentration is decreased in colonic mucosa with epithelial barrier damage [55,56], similar to the irradiated epithelium in our minipig model. Riveras et al. found that small intestine damage is involved with decreased MT and TJ defects in patients with cholesterol gallstone disease [57]. In this study, we examined the role of MT1/2 against radiation-induced enteropathy in the epithelial barrier. Exogenous MT1/2 internalizes in epithelial cells of the intestines, tubular cells of kidneys, and central nervous system (e.g., neurons, astrocytes, and microglia) via megalin receptors; it acts in detoxification, microglia inactivation, and neuron regeneration [37,38,58]. In irradiated conditions, application of exogenous MT1 or MT2 enhanced epithelial integrity and expression of junction molecules in vitro. MT2 was more effective than MT1 at alleviating epithelial damage and inhibiting p38 MAPK activation. We used MT2-deficient Caco-2 cells and siRNA mediated gene silencing to reveal the relationship between PS and MT2 in epithelial junction formation and epithelial permeability. Radiation-induced impairment of barrier integrity and intercellular junctions in MT2-deficient epithelial cells was not restored by PS treatment. Further PS did not suppress p38 MAPK activation in MT2-deficient epithelial cells. We found that MT2 was the downstream molecule of PS for regulation of epithelial integrity in irradiated conditions. However, the mechanism by which MT2 production is stimulated by PS needs to be elucidated further. The mouse model revealed that application of MT2 resulted in improvement in barrier function with inhibition of bacterial translocation to internal organs and alleviation of radiation-induced enteropathy. Taken together, these results indicated that MT2 is a novel therapeutic target for radiation-induced enteropathy.

In summary, we found that PS regulated intercellular junction formation and epithelial permeability in radiation-induced intestinal damage. PS mediated MT2 production, inhibited p38 MAPK, and reinforced junction formation and epithelial permeability. Activation of MT2 by chemicals such as PS may have therapeutic potential for alleviating conditions in which epithelial barrier formation is compromised by irradiation. These results indicated that PS reinforced epithelial integrity by modulating MT2 in radiation-induced epithelial damage. Maintenance of epithelial integrity is a novel therapeutic target for radiation-induced GI damage.

## Contributiors

Seo Young Kwak: Study design, collection and assembly of data, data analysis and interpretation, manuscript writing, critical reading and revision.

Won Il Jang; Study design, critical reading and revision

Seungwoo Park: Experimental material support, critical reading and revision

Sang Sik Cho; Collection and assembly of data, critical reading and revision

Seung Bum Lee: Collection and assembly of data, data analysis and interpretation, critical reading and revision

Min-Jung Kim: Collection and assembly of data, data analysis and interpretation, critical reading and revision

Sunhoo Park: Study design, experimental material support, critical reading and revision

Sehwan Shim: Study design, collection and assembly of data, data analysis and interpretation, critical reading and revisiontext= Hyosun Jang: Study design, collection and assembly of data, data analysis and interpretation, manuscript writing, critical reading and revision, and final approval of the manuscript

## Data sharing statement

The data that support the findings of this study are available from the corresponding authors, Hyosun Jang and Sehwan Shim, upon request.

## Declaration of Competing Interest

There are no conflicts of interest to declare.

## Acknowledgments

We thank Sun-Joo Lee and Hyewon Kim for their kind help with histological staining and analysis and Won-Suk Jang for his kind help with the minipig experiments. This research was supported by a grant from the Korea Institute of Radiological and Medical Sciences (KIRAMS), funded by the Ministry of Science and ICT (MSIT), Republic of Korea (grant numbers 50535-2021 and 50612-2021). This research was also supported by a grant from the National Research Foundation of Korea (NRF), funded by the Ministry of Science and ICT (MSIT), Republic of Korea (grant number 2020R1C1C1012154).

## Supplementary materials

Supplementary material associated with this article can be found in the online version at doi:10.1016/j.ebiom.2021.103641.

## References

[1] Peterson LW, Artis D. Intestinal epithelial cells: regulators of barrier function and immune homeostasis. Nat Rev Immunol 2014;14(3):141–53.
[2] Schulzke JD, Ploeger S, Amasheh M, Fromm A, Zeissig S, Troeger H, et al. Epithelial tight junctions in intestinal inflammation. Ann N Y Acad Sci 2009;1165:294–300.
[3] Citalán-Madrid AF, Vargas-Robles H, García-Ponce A, Shibayama M, Betanzos A, Nava P, et al. Cortactin deficiency causes increased RhoA/ROCK1-dependent actomyosin contractility, intestinal epithelial barrier dysfunction, and disproportionately severe DSS-induced colitis. Mucosal Immunol 2017;10(5):1237–47.
[4] Irvine EJ, Marshall JK. Increased intestinal permeability precedes the onset of Crohn's disease in a subject with familial risk. Gastroenterology 2000;119(6):1740–4.
[5] Katz KD, Hollander D, Vadheim CM, McElree C, Delahunty T, Dadufalza VD, et al. Intestinal permeability in patients with Crohn's disease and their healthy relatives. Gastroenterology 1989;97(4):927–31.
[6] Stacey R, Green JT. Radiation-induced small bowel disease: latest developments and clinical guidance. Ther Adv Chronic Dis 2014;5(1):15–29.
[7] Macià IGM, Lucas Calduch A, López EC. Radiobiology of the acute radiation syndrome. Rep Pract Oncol Radiother 2011;16(4):123–30.
[8] Dubois A, Walker RI. Prospects for management of gastrointestinal injury associated with the acute radiation syndrome. Gastroenterology 1988;95(2):500–7.
[9] Wang A, Ling Z, Yang Z, Kiela PR, Wang T, Wang C, et al. Gut microbial dysbiosis may predict diarrhea and fatigue in patients undergoing pelvic cancer radiotherapy: a pilot study. PLoS One 2015;10(5):e0126312.
[10] Shukla PK, Gangwar R, Manda B, Meena AS, Yadav N, Szabo E, et al. Rapid disruption of intestinal epithelial tight junction and barrier dysfunction by ionizing radiation in mouse colon in vivo: protection by N-acetyl-l-cysteine. Am J Physiol Gastrointest Liver Physiol 2016;310(9):G705–15.
[11] Nejdfors P, Ekelund M, Weström BR, Willén R, Jeppsson B. Intestinal permeability in humans is increased after radiation therapy. Dis Colon Rectum 2000;43(11):1582–7 discussion 7-8.
[12] Nakamura H, Arakawa K, Itakura H, Kitabatake A, Goto Y, Toyota T, et al. Primary prevention of cardiovascular disease with pravastatin in Japan (MEGA Study): a prospective randomised controlled trial. Lancet 2006;368(9542):1155–63.
[13] Jang H, Lee J, Park S, Myung H, Kang J, Kim K, et al. Pravastatin Attenuates Acute Radiation-Induced Enteropathy and Improves Epithelial Cell Function. Front Pharmacol 2018;9:1215.
[14] Jang H, Kwak SY, Park S, Kim K, Kim YH, Na J, et al. Pravastatin Alleviates Radiation Proctitis by Regulating Thrombomodulin in Irradiated Endothelial Cells. Int J Mol Sci 2020;21(5).
[15] Haydont V, Bourgier C, Pocard M, Lusinchi A, Aigueperse J, Mathé D, et al. Pravastatin Inhibits the Rho/CCN2/extracellular matrix cascade in human fibrosis explants and improves radiation-induced intestinal fibrosis in rats. Clin Cancer Res 2007;13(18 Pt 1):5331–40.
[16] Haydont V, Gilliot O, Rivera S, Bourgier C, François A, Aigueperse J, et al. Successful mitigation of delayed intestinal radiation injury using pravastatin is not associated with acute injury improvement or tumor protection. Int J Radiat Oncol Biol Phys 2007;68(5):1471–82.
[17] Wedlake LJ, Silia F, Benton B, Lalji A, Thomas K, Dearnaley DP, et al. Evaluating the efficacy of statins and ACE-inhibitors in reducing gastrointestinal toxicity in patients receiving radiotherapy for pelvic malignancies. Eur J Cancer 2012;48(14):2117–24.
[18] Sasaki M, Bharwani S, Jordan P, Joh T, Manas K, Warren A, et al. The 3-hydroxy-3-methylglutaryl-CoA reductase inhibitor pravastatin reduces disease activity and inflammation in dextran-sulfate induced colitis. J Pharmacol Exp Ther 2003;305(1):78–85.
[19] Klaassen CD, Liu J. Metallothionein transgenic and knock-out mouse models in the study of cadmium toxicity. J Toxicol Sci 1998;23(Suppl 2):97–102.
[20] Sato M, Bremner I. Oxygen free radicals and metallothionein. Free Radic Biol Med 1993;14(3):325–37.
[21] Takano H, Satoh M, Shimada A, Sagai M, Yoshikawa T, Tohyama C. Cytoprotection by metallothionein against gastroduodenal mucosal injury caused by ethanol in mice. Lab Invest 2000;80(3):371–7.
[22] Haq F, Mahoney M, Koropatnick J. Signaling events for metallothionein induction. Mutat Res 2003;533(1-2):211–26.
[23] Ferrario C, Lavagni P, Gariboldi M, Miranda C, Losa M, Cleris L, et al. Metallothionein 1G acts as an oncosupressor in papillary thyroid carcinoma. Lab Invest 2008;88(5):474–81.
[24] Inoue K, Takano H, Shimada A, Wada E, Yanagisawa R, Sakurai M, et al. Role of metallothionein in coagulatory disturbance and systemic inflammation induced by lipopolysaccharide in mice. Faseb j 2006;20(3):533–5.
[25] Inoue K, Takano H, Kaewamatawong T, Shimada A, Suzuki J, Yanagisawa R, et al. Role of metallothionein in lung inflammation induced by ozone exposure in mice. Free Radic Biol Med 2008;45(12):1714–22.
[26] Guo JZ, Wang WH, Li LF, Yang SM, Wang J. The role of metallothionein in a dinitrofluorobenzene-induced atopic dermatitis-like murine model. Sci Rep 2018;8(1):11129.
[27] Sambuy Y, De Angelis I, Ranaldi G, Scarino ML, Stammati A, Zucco F. The Caco-2 cell line as a model of the intestinal barrier: influence of cell and culture-related factors on Caco-2 cell functional characteristics. Cell Biol Toxicol 2005;21(1):1–26.
[28] Schlegel N, Meir M, Heupel WM, Holthöfer B, Leube RE, Waschke J. Desmoglein 2-mediated adhesion is required for intestinal epithelial barrier integrity. Am J Physiol Gastrointest Liver Physiol 2010;298(5):G774–83.
[29] van der Laan JW, Brightwell J, McAnulty P, Ratky J, Stark C. Regulatory acceptability of the minipig in the development of pharmaceuticals, chemicals and other products. J Pharmacol Toxicol Methods 2010;62(3):184–95.
[30] Shim S, Jang WS, Lee SJ, Jin S, Kim J, Lee SS, et al. Development of a new minipig model to study radiation-induced gastrointestinal syndrome and its application in clinical research. Radiat Res 2014;181(4):387–95.
[31] Paterson BM, Lammers KM, Arrieta MC, Fasano A, Meddings JB. The safety, tolerance, pharmacokinetic and pharmacodynamic effects of single doses of AT-1001 in coeliac disease subjects: a proof of concept study. Aliment Pharmacol Ther 2007;26(5):757–66.
[32] Gopalakrishnan S, Durai M, Kitchens K, Tamiz AP, Somerville R, Ginski M, et al. Larazotide acetate regulates epithelial tight junctions in vitro and in vivo. Peptides 2012;35(1):86–94.
[33] Haegebarth A, Clevers H. Wnt signaling, lgr5, and stem cells in the intestine and skin. Am J Pathol 2009;174(3):715–21.
[34] Srinivasan B, Kolli AR, Esch MB, Abaci HE, Shuler ML, Hickman JJ. TEER measurement techniques for in vitro barrier model systems. J Lab Autom 2015;20(2):107–26.
[35] Peerapen P, Thongboonkerd V. p38 MAPK mediates calcium oxalate crystal-induced tight junction disruption in distal renal tubular epithelial cells. Sci Rep 2013;3:1041.
[36] Meir M, Burkard N, Ungewiß H, Diefenbacher M, Flemming S, Kannapin F, et al. Neurotrophic factor GDNF regulates intestinal barrier function in inflammatory bowel disease. J Clin Invest 2019;129(7):2824–40.
[37] Langelueddecke C, Roussa E, Fenton RA, Thévenod F. Expression and function of the lipocalin-2 (24p3/NGAL) receptor in rodent and human intestinal epithelia. PLoS One 2013;8(8):e71586.
[38] Klassen RB, Crenshaw K, Kozyraki R, Verroust PJ, Tio L, Atrian S, et al. Megalin mediates renal uptake of heavy metal metallothionein complexes. Am J Physiol Renal Physiol 2004;287(3):F393–403.
[39] Chung RS, Hidalgo J, West AK. New insight into the molecular pathways of metallothionein-mediated neuroprotection and regeneration. J Neurochem 2008;104(1):14–20.
[40] Colleton C, Brewster D, Chester A, Clarke DO, Heining P, Olaharski A, et al. The Use of Minipigs for Preclinical Safety Assessment by the Pharmaceutical Industry: Results of an IQ DruSafe Minipig Survey. Toxicol Pathol 2016;44(3):458–66.
[41] Yao J, Guihard PJ, Wu X, Blazquez-Medela AM, Spencer MJ, Jumabay M, et al. Vascular endothelium plays a key role in directing pulmonary epithelial cell differentiation. J Cell Biol 2017;216(10):3369–85.
[42] Wilkinson EL, Sidaway JE, Cross MJ. Statin regulated ERK5 stimulates tight junction formation and reduces permeability in human cardiac endothelial cells. J Cell Physiol 2018;233(1):186–200.
[43] Turner JR. Intestinal mucosal barrier function in health and disease. Nat Rev Immunol 2009;9(11):799–809.
[44] Jørgensen VL, Nielsen SL, Espersen K, Perner A. Increased colorectal permeability in patients with severe sepsis and septic shock. Intensive Care Med 2006;32(11):1790–6.
[45] Laukoetter MG, Nava P, Nusrat A. Role of the intestinal barrier in inflammatory bowel disease. World J Gastroenterol 2008;14(3):401–7.
[46] Barmeyer C, Schulzke JD, Fromm M. Claudin-related intestinal diseases. Semin Cell Dev Biol 2015;42:30–8.

[47] Turner JR, Buschmann MM, Romero-Calvo I, Sailer A, Shen L. The role of molecular remodeling in differential regulation of tight junction permeability. Semin Cell Dev Biol 2014;36:204–12.
[48] Wang S, Gu J, Xu Z, Zhang Z, Bai T, Xu J, et al. Zinc rescues obesity-induced cardiac hypertrophy via stimulating metallothionein to suppress oxidative stress-activated BCL10/CARD9/p38 MAPK pathway. J Cell Mol Med 2017;21(6):1182–92.
[49] Kang YJ, Zhou ZX, Wang GW, Buridi A, Klein JB. Suppression by metallothionein of doxorubicin-induced cardiomyocyte apoptosis through inhibition of p38 mitogen-activated protein kinases. J Biol Chem 2000;275(18):13690–8.
[50] Takano H, Inoue K, Yanagisawa R, Sato M, Shimada A, Morita T, et al. Protective role of metallothionein in acute lung injury induced by bacterial endotoxin. Thorax 2004;59(12):1057–62.
[51] Ashino T, Arima Y, Shioda S, Iwakura Y, Numazawa S, Yoshida T. Effect of interleukin-6 neutralization on CYP3A11 and metallothionein-1/2 expressions in arthritic mouse liver. Eur J Pharmacol 2007;558(1-3):199–207.
[52] Pedersen DS, Fredericia PM, Pedersen MO, Stoltenberg M, Penkowa M, Danscher G, et al. Metallic gold slows disease progression, reduces cell death and induces astrogliosis while simultaneously increasing stem cell responses in an EAE rat model of multiple sclerosis. Histochem Cell Biol 2012;138(5):787–802.
[53] Mita M, Satoh M, Shimada A, Okajima M, Azuma S, Suzuki JS, et al. Metallothionein is a crucial protective factor against Helicobacter pylori-induced gastric erosive lesions in a mouse model. Am J Physiol Gastrointest Liver Physiol 2008;294(4):G877–84.
[54] Tsuji T, Naito Y, Takagi T, Kugai M, Yoriki H, Horie R, et al. Role of metallothionein in murine experimental colitis. Int J Mol Med 2013;31(5):1037–46.
[55] Mulder TP, Verspaget HW, Janssens AR, de Bruin PA, Peña AS, Lamers CB. Decrease in two intestinal copper/zinc containing proteins with antioxidant function in inflammatory bowel disease. Gut 1991;32(10):1146–50.
[56] Kruidenier L, Kuiper I, Van Duijn W, Mieremet-Ooms MA, van Hogezand RA, Lamers CB, et al. Imbalanced secondary mucosal antioxidant response in inflammatory bowel disease. J Pathol 2003;201(1):17–27.
[57] Riveras E, Azocar L, Moyano TC, Ocares M, Molina H, Romero D, et al. Transcriptomic profiles reveal differences in zinc metabolism, inflammation, and tight junction proteins in duodenum from cholesterol gallstone subjects. Sci Rep 2020;10(1):7448.
[58] Leung JYK, Bennett WR, King AE, Chung RS. The impact of metallothionein-II on microglial response to tumor necrosis factor-alpha (TNF$\alpha$) and downstream effects on neuronal regeneration. J Neuroinflammation 2018;15(1):56.